

BIORESORBABLE MULTIDRUG DELIVERY
CONDUIT TO PROMOTE PERIPHERAL
NERVE REGENERATION

by

Scott Ho

A thesis submitted to the faculty of
The University of Utah
in partial fulfillment of the requirements for the degree of

Master of Science

Department of Mechanical Engineering
The University of Utah

August 2016

Copyright © Scott Ho 2016

All Rights Reserved

The University of Utah Graduate School

STATEMENT OF THESIS APPROVAL

The thesis of Scott Ho
has been approved by the following supervisory committee members:

<u>Bruce Kent Gale</u>	, Chair	<u>10/26/15</u> Date Approved
<u>Jayant Prasad Agarwal</u>	, Member	<u>10/26/15</u> Date Approved
<u>Kenneth LaVann Monson</u>	, Member	<u>10/26/15</u> Date Approved

and by Timothy Ameal, Chair of
the Department of Mechanical Engineering

and by David B. Kieda, Dean of The Graduate School.

ABSTRACT

Peripheral nerve lesions caused by trauma often require the removal of the injured segment of nerve and subsequent repair by surgery. Nerve injuries that produce large gaps require a “bridge” to guide axon growth and reinnervation. Harvested autografts are currently the gold standard for bridging that gap but they have drawbacks including donor site morbidity, limited donor sites, and inconsistent efficacy. Surgically implanting a nerve guidance conduit is an alternative solution to grafting nerve conduits and such devices are presently available. However, many of them suffer from significant drawbacks such as nondegradable properties, nerve compression, complex fabrication techniques, and a lack of versatility in exchanging drugs. A bioresorbable multidrug delivery conduit that relies on the mechanics of diffusion has been developed to bridge the nerve gap and locally deliver neurotrophins and other regeneration promoting drugs to the regeneration site. Conduit design, drug delivery modelling, manufacturing techniques, and release verification testing will be discussed.

This work is dedicated to my family, present and future, for whom I will spend my talents and efforts to make their dreams a possibility. “People are more important than possessions, problems, and getting things done.”

TABLE OF CONTENTS

ABSTRACT.....	iii
LIST OF FIGURES	vii
ACKNOWLEDGEMENTS.....	viii
CHAPTERS	
1. BACKGROUND	1
1.1. Neurotrophic Factors and Other Drugs	2
1.2. Nerve Grafting.....	3
1.3. Guidance Conduits	4
1.4. Local Delivery of Regeneration-Promoting Drugs	5
1.5. Material Selection.....	6
1.6. Prior Work.....	7
1.6.1. Initial Diffusion Model	8
1.6.2. PDMS Conduit Delivery Devices	8
1.6.3. PLGA Conduit Delivery Devices	9
1.7. Conduit Improvement and Innovative Work.....	9
1.8. Thesis Overview.....	10
2. MULTIDRUG DELIVERY CONDUIT.....	12
2.1. Diffusion Modelling.....	12
2.1.1. Theory: Fick's Diffusion.....	12
2.1.2. Numerical Model	13
2.1.3. Delivery Parameters.....	14
2.1.4. Modelling Results	16
2.2. Manufacturing Methodology.....	18
2.2.1. Material Fabrication.....	19
2.2.2. Assembly Material	19
2.2.3. Conduit Assembly.....	21
2.2.4. Sterilization	22
2.3. Device Verification Methodology: Release Kinetics	23
2.3.1. Dual Conduit Zeroth-Order Release Test	25
2.3.2. Single-Conduit 60% over 30 Days Dextran Release Test	26
2.3.3. Single Conduit NGF Release Test	26

2.3.4. Single Conduit Dextran Release Test at Simulated <i>in vivo</i> Conditions.....	27
2.4. Release Results and Discussion	28
2.4.1. Dual Conduit Zeroth-Order Release Test	28
2.4.2. Single-Conduit 60% over 30 Days Dextran Release Test	29
2.4.3. Single Conduit NGF Release Test	30
2.4.4. Single Conduit Dextran Release Test at Simulated <i>in vivo</i> Conditions.....	32
3. SUPPORT MATERIALS	34
3.1. Diffusion Hole Stability	34
3.1.1. Hole Processing	36
3.1.2. Hole Stabilization Conclusions.....	40
3.2. Sterilization	40
3.2.1. Sterrad	42
3.2.2. Ethylene Oxide.....	42
3.2.3. Ethanol	42
3.2.4. Sterilization Justification	44
4. CONCLUSIONS.....	45
4.1. Conclusions	45
4.1.1. Drug Release	46
4.1.2. Device Structure.....	47
4.2. Contributions	47
4.2.1. Modelling.....	47
4.2.2. PLGA Processing and Manufacturing	48
4.2.3. Release Kinetics.....	48
4.3. Future Work	48
APPENDIX: DIFFUSION MODEL – MATLAB CODE.....	51
REFERENCES	64

LIST OF FIGURES

1.1: Dual drug delivery mouse conduit.....	10
2.1: Diffusion model convergence with varying iterations.....	17
2.2: Conduit assembly - inner conduit, outer conduit, and end caps	19
2.3: Dual reservoir conduit assembly (stage 1 top, completed bottom).....	22
2.4: Zeroth-Order dextran release test using dual mouse conduits.....	28
2.5: 60% dextran release test using single rat conduits	29
2.6: NGF release test conducted in <i>in vivo</i> environment	30
2.7: NGF cumulative concentration diffusion	31
2.8: Dextran diffusion test conducted in <i>in vivo</i> environment.....	33
3.1: Diffusion hole shrinkage at 37°C a. after drilling b. 24 hours after being submersed in PBS c. 48 hours after being submersed in PBS	35
3.2: Laser-annealed hole after submersed in water at 37°C for a. 0 hours b. 8 hours c. 24 hours d. 72 hours.....	36
3.3: Heat-annealed hole after submersed in water at 37°C for a. 0 hours b. 8 hours c. 24 hours d. 72 hours.....	37
3.4: Plasma-processed hole after submersed in water at 37°C for a. 0 hours b. 8 hours c. 24 hours d. 72 hours.....	38
3.5: Punched hole after submersed in water at 37°C for a. 0 hours b. 8 hours c. 24 hours d. 72 hours.....	39
3.6: Sterrad presterilization hole and poststerilization hole.....	43
3.7: Ethylene oxide poststerilization deformation and sealed hole.....	43
3.8: Ethanol presterilization hole and poststerilization hole.....	43

ACKNOWLEDGEMENTS

There are innumerable people and organizations who contributed to the work presented in this thesis, many of them who go unnamed. I'd first like to thank Dr. Bruce Gale for his mentorship and guidance as both an advisor and mentor. He spent countless hours providing guidance and support during my years at the University of Utah. Thank you to Dr. Jay Agarwal who served as principal investigator to this project as well as Dr. Jill Shea, Dr. Himanshu Sant, and fellow students Keng-Min Lin, Pratima Labroo, and Megan Roach who directly aided in many aspects of this project. Additional thanks to Jeremy Riley for aid in manufacturing.

This research was funded by the Department of Defense Congressionally Directed Medical Research Programs Discovery Award and Idea Development Award. I would like to thank the University of Utah and especially the Department of Mechanical Engineering and Department of Surgery for their faculty, staff, facilities, and equipment that made this research possible.

I'd like to give a special thanks to my family, friends, and mentors who helped me reach this point in my life and taught me the values of an education, hard work, and commitment to a greater good.

CHAPTER 1

BACKGROUND

Poor recovery from peripheral nerve injuries continues to be a major cause of life-long loss of function by the resulting nerve damage. A degeneration process known as Wallerian degeneration occurs at serious peripheral injury sites prior to the regeneration of nerve fibers [1]. The process involves fragmentation of axons and the myelin sheath, leaving behind a column of collapsed Schwann cells. These cells play a vital role in the following regeneration process by producing necessary neurotrophins such as nerve growth factor (NGF) that aid the healing process. Minimizing the period of degeneration is essential to successful functional recovery. As the regeneration process begins, axon endings use the Schwann cells as guides to complete the reinnervation process.

However, serious injuries that result from laceration of peripheral nerves often result in a nerve gap greater than one centimeter following the nerve degeneration process. In such cases, regenerating axons are no longer restricted to their original sheaths and they lose their natural guides, allowing them to wander into surrounding tissue. The consequence is often failed reinnervation of the necessary organs and tissues resulting from incomplete neurological recovery. Regenerating axons may successfully bridge these long gaps spontaneously on occasion. However, creating a guide, whether a nerve graft or artificial conduit can greatly minimize the amount of scarring that occurs and significantly increase the odds for successful recovery. The reinnervation process

requires both physical and cell signal guidance to ensure proper growth.

The success of return of function to organs following reinnervation is time-sensitive. Many of the end organs can undergo their own degeneration and muscle fibers atrophy by ~70% in cross-sectional area by two months after nerve severance. Motor endplates typically will be preserved at least a year after denervation. As a result, it is vital that the reinnervation process occur as quickly as possible.

1.1. Neurotrophic Factors and Other Drugs

Traditionally, axon regeneration rates have been assumed to be fairly constant at 1mm per day. However, regeneration tests under various factors have reported a spectrum of rates varying from as low as 0.5mm per day up to 9mm per day. While some of this variation can be attributed to location relative to the proximal and distal stumps and varying measurement techniques, a key factor to the success of the regeneration process is the presence of essential neurotrophins and growth factors. Neurotrophins such as NGF have been identified as cell-signaling molecules that have the ability to guide axons as they grow [2]. Additionally, they provide a stimulus for growth of advancing axons and studies have shown significant increase in growth rates with the presence of these growth factors [3]. One study shows that when sciatic nerve segments are exposed within a bioactive range of 5-50ng/mL of NGF, there are significant improvements to the fiber density and width [4]. An alternate study indicated that there were synergistic effects in combining glial cell line-derived neurotrophic factor (GDNF) and NGF [5]. When dorsal root ganglion (DRG) cells were treated with these factors within a range of 0.1ng/mL to 10ng/mL, the resulting cells showed significant length and density growth improvements.

Alternate drugs have also shown promise in the nerve regeneration process.

Tacrolimus (FK506) is a common immunosuppressant drug, but it has also been tested in sciatic nerve repair [6]. While tacrolimus showed marginal benefit in the reinnervation process, it displayed significant benefits to functional recovery after reinnervation. Some studies have even seeded artificial nerve guides with Schwann cells to guide axons and improve the regeneration process [7]. Assisted delivery of such drugs or cellular transplants will be essential in returning full function to peripheral nerve injury sites. There is still much debate about optimal drug and growth factor selections to promote nerve regeneration. Consequently, developing a delivery vehicle that can easily alternate drugs based on bioactivity results will greatly accelerate peripheral nerve injury research.

1.2. Nerve Grafting

In cases where the nerve lesion is too large to suture the nerve endings together without tension, autologous nerve grafts have been seen as a standard of care. The procedure involves harvesting nerve tissue from other locations on the body and reconstructing the injured section. While these grafts dramatically improve the chances of successful recovery compared to an untreated injury, they do have significant downsides. First, they require a donor site; autologous nerve grafts are often elected over allografts to reduce the risk of a negative autoimmune response. The result is an additional injury that must heal and regain function and there are limited harvest sites available and no guarantees that the donor graft will support axonal regeneration [8]. In addition, larger nerve grafts require additional tissue and ideal donor sites of the required volume are often lacking. There have been attempts to synthesize a combination of natural and synthetic grafting techniques. In one study, chemically extracted acellular allogenic nerve grafts that were implanted with autologous mesenchymal stem cells revealed functional

recovery after 6 months and results comparable to autologous nerve grafts [9]. These hybrid grafts were able to introduce a secondary donor site to the autograft and provide sufficient tissue to fill the injury site. However, the introduction of foreign tissue and possibility of rejection required the use of immunosuppressive agents, significantly increasing the risk of infection and other systemic effects. While grafts have been shown to provide a feasible option to bridge a nerve lesion, they do have drawbacks that drive the need for more innovative solutions.

1.3. Guidance Conduits

An alternative solution to tissue grafts is providing a guidance conduit to promote axon innervation. These conduits are surgically implanted into the donor site and act as a bridge between the nerve endings. Being able to fabricate conduits to site-specific geometries offers significant benefits to autografts which depend on the available donor tissue. Nerve guidance conduits are currently commercially available and research on these devices has been ongoing since the 1980s. Studies have shown that these conduits provided mechanically stable structures that are easily sterilized and performed their engineering functions. The earliest clinical attempts of using silicone tubes provided a path for the nerve axons to regenerate and connect with their distal stumps [10]. However, one problem that plagued nonresorbable devices such as these was a compression of the nerve and tension at the suture sites following reinnervation. Another study used devices constructed of poly-vinyl alcohol (PVA), a material that is easily sterilized and able to successfully reinnervate a nerve lesion. [11]. Again, the problems occur as the reinnervated injury grows in tissue mass; the conduit is no longer needed but the only solution to remove the now restricting conduit is through surgery. The need to

remove the device in a later operation greatly reduces the appeal of nondegradable devices. Conduits constructed of bioresorbable materials avoid this issue by degrading within the body through natural mechanisms over time. These conduits can be made of natural or synthetic material. To demonstrate one example, collagen conduits are commercially available and have been shown to repair nerve gaps up to 20mm [12]. Nonetheless, because these conduits can take up to 48 months to degrade, similar compression problems that persist in nondegradable conduits persist. While a secondary surgery is not required to remove the device because it can be fully resorbed after the material lifetime, regeneration of the lesion site is not ideal.

Polyglycolic acid (PGA) conduits provide a dramatically decreased degradation time compared to collagen conduits; the material maintains structural integrity for 1-2 months and loses total mass in a little over 6 months. Yet, existing devices encountered poor functional motor recovery from these devices. The reduced degradation time ended up being a key limitation to the recovery process as mechanical properties were lost before the proximal and distal stumps could reconnect. Literature has shown that there have been many attempts to optimize degradation rates by testing various materials. An ideal balance lies in providing mechanical stability while the nerve is regenerating, but then allowing for expansion and tissue growth once innervation occurs.

1.4. Local Delivery of Regeneration-Promoting Drugs

Introduction of neurotrophic factors during the reinnervation process in conjunction with bioresorbable conduits has the potential to provide the physical and signal guidance that nerve axons require to regenerate properly. Polylactic-co-glycolic acid (PLGA) has been a highly attractive polymer for drug delivery. The majority of current nerve conduit

devices using PLGA consist of microsphere or nanosphere drug encapsulation techniques that incorporate its degradation process into the release of drugs to the nerve injury site [13]. These elegant designs have multiple fabrication methods, including emulsification-solvent evaporation, spray-drying, solvent-casting, and extrusion. Significant progress has been made in determining ideal parameters to produce a conduit that releases a specific drug and dosage effectively. However, many of these devices require manufacturing techniques that are not practical for large-scale production. Additionally, the complex processes involved in fabrication and tuning for specific drug release diminish the ability to alternate drugs without completely redesigning each conduit. There has been little progress in correlating release rate parameters with specific drug chemistry. As a result, these microsphere and nanosphere devices have not proven to be a feasible solution in the present nerve regeneration scope.

The status of drug delivery and axonal growth to promote peripheral nerve regeneration is still in a stage of optimization. While certain drugs provide significant benefits to growth rates and mass, it is still relatively unknown which of these drug combinations and dosages result in ideal regeneration. This statement is especially valid for local drug delivery. As a result, nerve conduit development is as much of a search for a clinical device as it is for a research device to help identify optimal pharmaceuticals for local delivery.

1.5. Material Selection

In addition to the materials discussed above, other materials that have been used to build functional nerve guidance conduits include polycaprolactone (PCL), polyhydroxybutyrate (PHB), polyurethane, chitosan, fibrin, silk, and others [14].

Biopolymers provide biocompatible characteristics and can often tailor mechanical properties that are complimentary to the regenerating nerve. Alternatively, synthetic materials, while not immediately as biocompatible, provide further opportunity to tune parameters such as degradation rate, porosity, and microstructure. Additional mechanical properties that have been taken into consideration are tensile strength, suturability, surface chemistry, and ease to embed bioactive cues into the conduits.

Poly(lactic-glycolic acid) (PLGA) is a highly favored synthetic polymer because of its long clinical experience, tunable degradation characteristics, and ability to sustain long-term delivery methods. The material undergoes hydrolysis of ester linkages in water and breaks down into lactic acid/glycolic acid. Both of these original monomers are by-products of natural metabolic processes so the body can effectively deal with them. PGA can be converted to metabolites by the body and PLA can be cleared through the tricarboxylic acid cycle [15]. A vital characteristic of PLGA is its controllable degradation rate. Depending on the PLA-PGA ratio, the half-life of the copolymer can vary from 6 months down to 2 weeks [16]. The appropriate degradation rate can be chosen depending on a target delivery period in addition to the material's degradation during the conduits' manufacturing and processing time. PLGA has been used extensively in the development of nanosphere drug delivery so we know it has favorable properties likely to deliver the bioactive cues and growth factors we desire.

1.6. Prior Work

The work discussed in this thesis is in continuation to prior work performed in Dr. Jay Agarwal's and Dr. Bruce Gale's lab by Keng-Min Lin [17]. This section will highlight key methods and outcomes from the result of that work.

1.6.1. Initial Diffusion Model

A diffusion model based on Fick's Diffusion was developed to predict the drug release behavior of the nerve conduits. The theory and construct of the model will be discussed later in the modelling section. This model provided an expected diffusion rate that device release rates were benchmarked against. Shortcomings to the existing diffusion model were primarily due to the fact that this model was constructed in a manner that had to be rebuilt every time an input parameter was changed. This model also did not explore comparisons between *in vitro* collection concentrations and *in vivo* exposure concentrations of the drugs being delivered.

1.6.2. PDMS Conduit Delivery Devices

This project initially tested devices constructed of polycarbonate-urethane (PCU) and poly-di-methyl-siloxane (PDMS). A PCU tube was heat extruded and then cut to length to form the guidance conduit and a PDMS drug reservoir was constructed around it. The behavior and manufacturing techniques with PDMS are well known and these tests explored the difference between diffusion through a permeable membrane vs. diffusion through controlled holes. The membranes tested were constructed of polyethersulfone (PES). A series of release tests was performed with these devices and the results showed that devices with the PES membrane had a higher diffusion rate than the diffusion hole. In addition, the diffusion patterns between devices with and without membranes was very similar. Both of them had a significant initial burst, regardless of the target diffusion rate. As a result, it was concluded that using a diffusion membrane did not contribute to sustaining a consistent extended release.

1.6.3. PLGA Conduit Delivery Devices

In continuing the development of PDMS devices, devices were fabricated from PLGA as well. A molding process was used to produce the conduit and drug reservoir. First, PLGA pellets were dissolved in an acetone-ethanol emulsion and then molded into tubes. They were then cut to size and placed concentric to one another. The ends were sealed to form a drug reservoir between the two lumens. A detailed process of the updated and refined manufacturing techniques will be described later in the manufacturing methodology section. The sealing of the device reservoirs required the use of nondegradable sealants and was not fully bioresorbable, but it suited the functions necessary to test the release kinetics of the device. Release from these devices showed similar release patterns to the PDMS devices, with a large initial burst effect. However, the deviations between tests were significant and prompted the need to improve the reliability of drug release. These devices all consisted of a single drug reservoir to deliver an individual drug to the injury site.

1.7. Conduit Improvement and Innovative Work

The work in this thesis proposes new manufacturing techniques and functional improvements to nerve conduits and continues on the prior work done in Dr. Jay Agarwal's and Dr. Bruce Gale's labs. There are major benefits in providing a guidance conduit that can independently deliver multiple localized drugs to the injury site. Additionally, there has not been enough testing performed to understand the unknown effects of combining multiple drugs together in the delivery reservoir so a dual reservoir system will provide a delivery system for multiple drugs until these effects are studied. A bulk diffusion delivery device will provide flexibility in easily alternating drugs as well

as precision in using traditional fluid mechanics to control delivery rather than complex polymer degradation (Figure 1.1).

1.8. Thesis Overview

This thesis explains the derivation and dependencies that were demonstrated in the diffusion model. The model was then used to benchmark diffusion kinetic release tests. The fabrication methodology will discuss the refinement of PLGA conduit formation, end cap formation, and solvent welding of the drug reservoirs. Additional manufacturing techniques that were developed to drill diffusion holes and minimize PLGA's dynamic properties when exposed to sterilization, hydrolysis, and *in vivo* conditions are also discussed. A series of four diffusion tests that were conducted to verify drug delivery

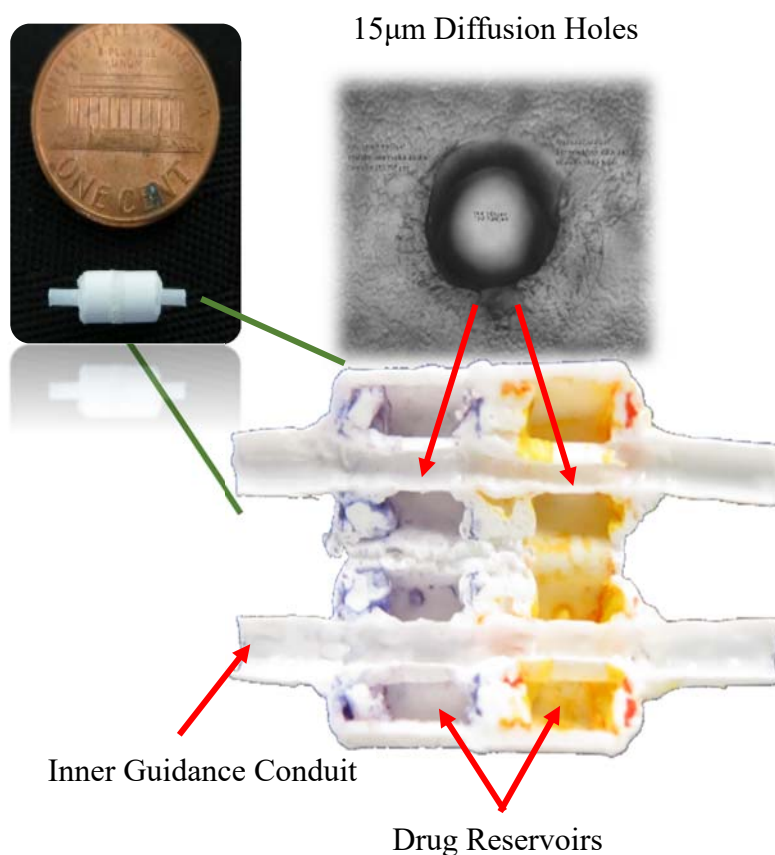


Figure 1.1 Dual drug delivery mouse conduit

from the nerve conduits will be summarized and the analysis, results, and conclusion will provide a clearer justification as to whether diffusion is a reliable delivery method for peripheral nerve regeneration. PLGA's suitability and challenges that arise from using this untraditional engineering polymer in this type of conduit device is also detailed. Overall, the efficacy of drug delivery through a PLGA device that uses diffusion holes to administer a prolonged drug release to guide and reinnervate peripheral nerves was explored.

CHAPTER 2

MULTIDRUG DELIVERY CONDUIT

2.1. Diffusion Modelling

Using basic diffusion as the primary mode of drug release has been relatively unexplored for peripheral nerve injuries. Drug delivery rates from devices are dependent on geometric factors as well as the diffusion coefficients of drugs supplied. This approach provides a much simpler release model for a device that is designed to discharge drugs.

The original mathematical model developed to model the release of drugs from these devices was built with Microsoft Excel and worked with fixed iteration intervals. The primary improvements that were made from the existing model to the current model involved restructuring the model to a foundation of dependent variables that allows it to be adjusted with a selection of critical variables. The model was developed using MATLAB software.

2.1.1. Theory: Fick's Diffusion

Fick's 1st law relates a particle's diffusive flux to its concentration through the following relationship:

$$J = -D \frac{d\Phi}{dx}, \quad (\text{Equation 1})$$

where J is the diffusive flux $\left(\frac{ng}{cm^2 \cdot s}\right)$, D is the diffusion coefficient, Φ is the drug concentration, and x is the linear position.

Fick's second law relates change of concentration at a specific location over time as

$$\frac{d\phi}{dt} = D \frac{d^2\phi}{dx^2}. \quad (\text{Equation 2})$$

Under steady-state conditions, Fick's 2nd law simplifies into the first law. With the exception of the leveling of concentration gradient during the initial burst of drug release, it is safe to assume that our device releases at steady-state conditions and this holds true, simplifying the diffusion model.

2.1.2. Numerical Model

2.1.2.1. Model Design

Certain assumptions have to be made to consider the diffusion model valid. The first involves the design of the model. The model was constructed by simplifying the conduit in to three distinct regions: a uniform drug reservoir, the diffusion hole, and the inner conduit. In order to assume a one-directional diffusion, certain parameters must be met. First, the drug must be a homogenous solution, which means that the model ignores the effects of gravity and device orientation. Another assumption that is made in the model is that diffusion of drug occurs in a zero-velocity environment. Fluid motion can dramatically alter the performance of the device. The final crucial assumption that has to be made is that the nerve conduit remains a constant geometry device. The reservoir size cannot expand or collapse; if it did, it would produce fluid motion that would alter the release of drug. Additionally, because Fick's diffusion is dependent on the cross-sectional and length geometries of diffusion regions, results can vary if the device walls expand or contract.

Two different models were made: one to predict *in vitro* tests and one to predict *in vivo* behavior (APPENDIX). MATLAB software was used to produce the models. The

primary difference between the two is what dosage values are important in each case. The *in vitro* tests are measured in a receiver chamber, which collects the drug released from the system. At the time intervals where readings are collected, the receiver chambers are flushed and refilled with clean medium. This flushing process is accounted for in the model. The *in vivo* concentration of interest is the internal instantaneous concentration gradient within the guidance conduit. Under ideal conditions, this gradient will be linear within each diffusion region and is proportional to the diffusivity parameters of the sections. The model has the ability to correlate these two values to compare *in vitro* data with expected *in vivo* performance. The parameters that control this correlation will be discussed later.

2.1.2.2. Convergence

As with any numerical model, convergence of the results can affect the accuracy of the data. This model is a three-stage calculation that does not involve in-depth finite difference modelling or other methods that typically have high convergence thresholds. Because of this, we anticipated minimal errors and a convergence test was conducted to verify this. The convergence sensitivity was tested using 3, 10, and 100 iterations to validate whether the model avoided calculation errors.

2.1.3. Delivery Parameters

There are many parameters that affect the diffusion performance of drug delivery. One major advantage of this device is their independent behavior. First, the diffusion coefficient is determined by the specific drug being used and what medium it is diffusing through, with slight variations that depend on pressure and/or temperature. There are many theoretical calculations that can be used to determine this coefficient. One of the

simplest models is the Stokes-Einstein equation, where particles are assumed to be spherical and are diffusing through a viscous liquid continuum. This is a purely theoretical calculation that yields results that can vary by up to 40%. The Wilke-Chang equation relies on more empirical data and coefficients in its calculations, but it assumes that associated molecules behave as large-size molecules. The Scheibel equation calculates the diffusion coefficient by comparing molar volumes of particles and is accurate when the drug particle volume is smaller than the diffusion medium particle volume. While these theoretical calculations progressively become more accurate, the most accurate method of determining the coefficient of diffusion is to use experiments. Empirical measurements show the diffusion coefficient for NGF as $1.26 \times 10^{-6} \frac{\text{cm}^2}{\text{sec}}$ when flowing through a buffered solution [18].

2.1.3.1. Dimensional Analysis: Variable Dependencies

For our nerve conduit, the diffusion rate depends on a specific set of constants. The first one is diffusion coefficient. Fick's diffusion rate is linearly dependent on the drug diffusion coefficient and as a result, the rate of release will linearly change based on this value. The other factors that affect diffusion rate the most are the geometric parameters of the conduit. For each diffusion region, the cross-sectional area and length that it diffuses through affect the concentration gradient. As cross-sectional areas are decreased, the diffusion rate within each region is linearly decreased. Consequently, the conduit diameter and diffusion hole diameter will modify the diffusion rates in a quadratic manner. As length of the inner conduit and wall thickness are increased, the diffusion rates through each of their regions also increase by a linear relationship. Finally, the amount of drug available does not affect the diffusion rate, but it does scale the actual

concentrations that are delivered over a set time. This value is determined by reservoir volume and the initial concentration of drug loaded into each device. This combination of adjustable variable inputs allows for fine tuning of the drug delivery parameters.

Concentration measurements report the actual drug values accumulated in the receiver chamber or present in the conduit, depending on whether *in vitro* or *in vivo* tests are performed. These values essentially represent the integral of the diffusion rate and as a result, the measured concentration values are dependent on the rates of diffusion. For example, because initial concentration has a zeroth-order effect on diffusion rate, it has a first (linear) order effect on concentration dosage delivery values. While conduit length and wall thickness have a first-order effect on diffusion rate, they change concentration values in a quadratic relationship. The process of tuning diffusion rates to levels that will produce desired results is decided by modifying lesser-fixed variables to account for fixed variables. Diffusion hole size and initial concentration are the least-dependent variables that can be modified to compensate for the diffusion rate of each drug selected and the conduit size required.

2.1.4. Modelling Results

A convergence test was run to verify that the model produced data with minimal convergence errors and the results show that within 100 iterations, the model converges with <0.01% error (Figure 2.1). One factor that can multiply this error is the behavior for collection times to round the collection values to the closest time point. As a result, the actual model tests were run with two iterations each hour. Because the drug diffusion models were conducted using >700 iterations, the convergence error was declared insignificant to the accuracy of the model.

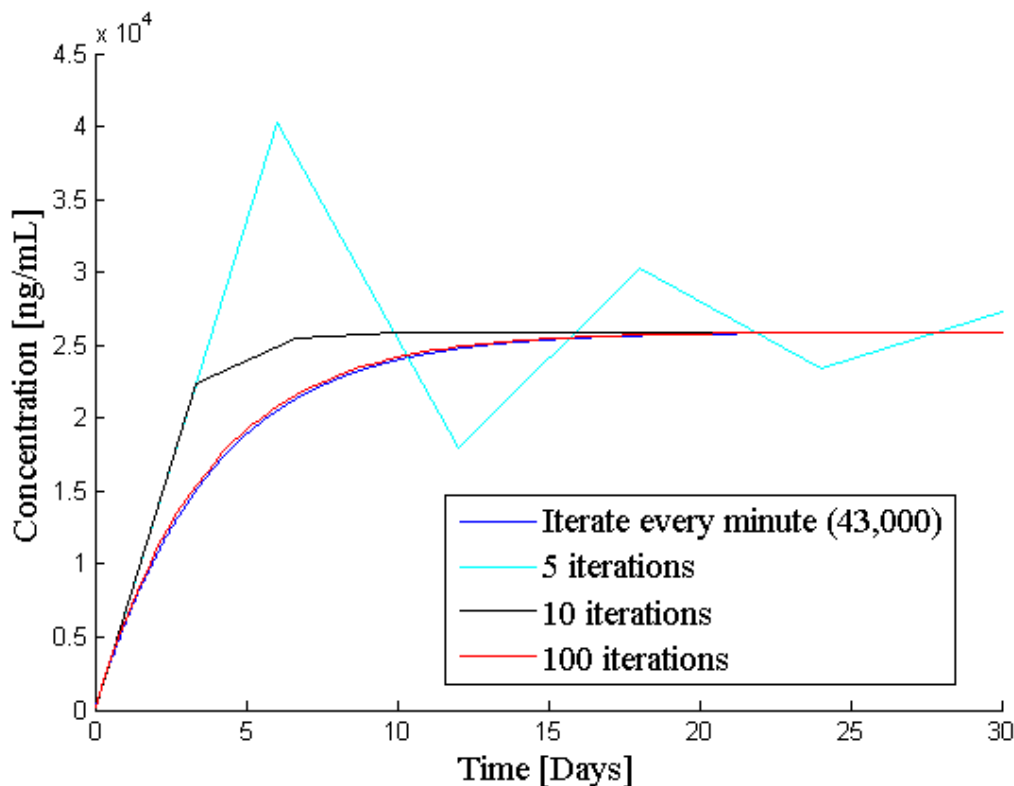


Figure 2.1: Diffusion model convergence with varying iterations

The diffusion model was used to determine parameters that would be used for each of the release kinetics tests proposed. Two primary diffusion targets were explored: maintaining a zeroth-order diffusion over 30 days and targeting a 60% release over 30 days. Preliminary dextran release tests targeted a linear release of drug and while the release is never truly linear, it was found that by maintaining a 5% release over 30 days, the release rate would change by <10% over that time interval.

By limiting diffusion to such a small range, safety concerns and flaws in manufacturing are amplified. First, in order to deliver the target concentrations, a significantly higher target concentration must be loaded into the conduits. In a worst-case scenario, if the device were to leak or burst within the body, the released drug could exceed toxicity levels. Additionally, as smaller diffusion holes are required to produce the

low diffusion ranges, in minor leaks and fluctuations based on manufacturing quality, device stability, and environmental variability can produce dramatically larger discrepancies than if a larger diffusion hole were used. With the *in vitro* tests, it is unknown whether the drug collected in the receiver chamber is released from the diffusion hole or if it is simply leaking from the device. If the diffusion hole can be made larger, the rate of diffusion through that proper channel becomes much larger than possible leaks and the data reliability and confidence increases. These reasons and the small differences between the diffusion hole and sealed devices in initial tests were enough to prompt a revised target diffusion range.

A 60% release over 30 days was selected as a revised target diffusion. Minimizing safety risks, manufacturing errors, and environmental effects were major factors leading to this decision. However, another conclusion that made this selection feasible is the bioactive range of many of our drugs of interest. NGF has been shown to be bioactive and efficacious from 0.1ng/mL up to 20ng/mL; that range provides a significant delivery range for this nerve conduit.

2.2. Manufacturing Methodology

The nerve conduit was designed to be bioresorbable to avoid a secondary surgery for removal of the device following the healing process. As such, PLGA was selected as the material of choice because of its widespread usage in other bioresorbable medical devices. This polymer provides the resorbable properties necessary for the device, but by being a degradable material, it presents some unique challenges that traditional engineering materials would otherwise avoid, including a low glass transition temperature (40-60°C) and nontraditional mechanical properties.

2.2.1. Material Fabrication

The bioresorbable guidance conduits were produced using 75/25 poly-lactic-glycolic-acid (PLGA; 7525 DLG 7E, Evonik). Two liquefying methods were explored: melting and dissolving PLGA. It was found that in melting the polymer, significant degradation had occurred in the material making it highly brittle and unworkable. The solvent method was selected for manufacturing devices and is detailed below.

The stock 75/25 PLGA pellets were dissolved in acetone at a ratio of 10g PLGA to 20mL acetone at 45°C. After manually stirring until a viscous solution formed, 6mL of ethanol was added to the solution. The ethanol serves as an emulsifier for the acetone to be displaced when the solution interacts with water. The solution was stirred at 180RPM on a stirring plate until visibly homogenous. The solution was then used to fill glass molds. A flat petri dish was used as the mold to form 1.5mm thick sheets and glass tubing of various sizes were filled to construct the PLGA conduit tubing.

2.2.2. Assembly Material

The nerve conduits are composed of three primary pieces: an inner guidance conduit, outer drug reservoir conduit, and the end caps to seal the construction (Figure 2.2).

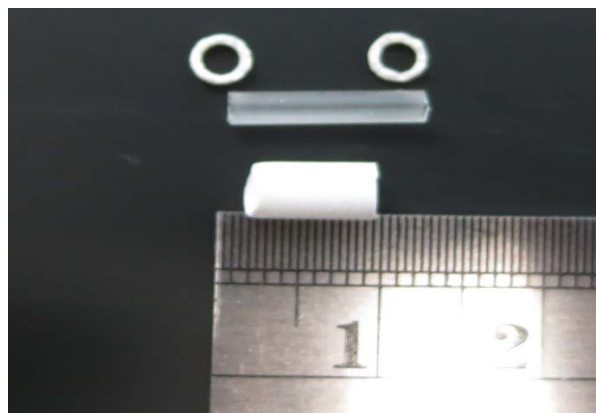


Figure 2.2: Conduit assembly - inner conduit, outer conduit, and end caps

Glass tubing was used to mold the conduits. For conduits smaller than 3mm inner diameter, the following procedure was used. PLGA solution was suctioned into glass molds and then frozen at -20°C for 24 hours. Following that, they were left to cure for 12 days at 23°C (room temperature). As the solvent evaporated from the solution, the surface tension from the mold naturally produced an even-thickness conduit within. The resulting thickness of the conduits is a factor that can be controlled based on the polymer-solvent ratio. Following the curing process, the conduits were manually broken out of the glass molds and an ultrasonic bath was used to remove any remaining glass.

For conduits larger than 3mm inner diameter, one additional processing step was taken to account for the decrease in surface tension forces due to the decreased surface area to volume ratio. Immediately following the suctioning of material into the conduits, any excess PLGA was allowed to drip out of the molds. The conduits were then placed vertically into a water bath and allowed to cure. The water bath quickly displaced the solvent and reduced deformations caused by gravity forces on the conduit. After 12 days, the conduits were released from the mold by using a matching ramrod to push them out.

Conduit dimensions were determined based on studies for sciatic nerve repair for rat and mouse models. The following dimensions were used. The mouse inner conduits were molded to dimensions of 1.25mm OD and 1.067mm ID and then cut to a length of 13mm. The rat inner conduits were molded to dimensions of 2.4mm OD and 2mm ID and also cut to a length of 13mm. The outer conduits were the same for both devices, measuring 4mm OD and 3mm ID and cut to a length of 7mm.

End caps to join the conduits and form the drug reservoir were manufactured by forming a PLGA sheet. The same PLGA solution that was used for the conduits was

poured on to a glass petri dish and left on a 45°C hot plate. This heating process cures the sheet in a bottom-up process that minimizes wrinkling of the sheet as it expands and contracts. Following 4 hours on a hot plate, the sheet was submerged into water, allowing the emulsion process to remove any remaining solvent. The end caps were cut to size using a laser cutter. A properly sized end cap creates a slight press fit over the inner conduit and within the outer conduit.

2.2.3. Conduit Assembly

A solvent bonding process was adopted to assemble and seal the PLGA conduits. A solution consisting of 2g PLGA and 2mL acetone was mixed together to form a viscous solution. The solution was locally applied to join the end caps to the inner conduit. Following each application of solvent glue, the devices were placed into a water bath for 24 hours to remove any residual solvents and return the assembly to a solid structural state. The resulting device is shown below in stage 1 of assembly (Figure 2.3).

After stage 1, diffusion holes are then drilled into the devices using laser milling. Holes larger than 100µm were drilled using a VLS3.60 CO₂ system (Universal Laser Systems) and holes smaller than 100µm were drilled using a MicroMaster KrF excimer laser system (Optec). The laser holes were stabilized by pulsing the laser multiple passes (40x). This process annealed the PLGA surrounding the diffusion holes and made them more stable once submersed into water.

The final assembly step involved solvent welding the outer conduits to complete the drug reservoir. For the tests involved, both single and dual reservoir devices were built using this process. Once the outer conduit was attached, the devices were again placed in a water bath to displace any remaining acetone.



Figure 2.3: Dual reservoir conduit assembly (stage 1 top, completed bottom)

2.2.4. Sterilization

PLGA poses a few problems regarding sterilization. It is a reactive polymer that may break down from certain radiation or chemical sterilization processes. Additionally, the fragile co-polymer has a very low melting point and even lower glass transition temperature (40-60°C), eliminating many traditional sterilization methods like autoclaving. A study that ran sterilization tests involving ethanol, ethylene oxide (ETO), and plasma sterilization has shown that plasma sterilization yields the best results regarding PLGA degradation and device sterility [19]. Additional sterilization tests involving PLGA conduits with diffusion holes were performed. Samples were sterilized using 70% ethanol (n=42), ETO (n=46), and a Sterrad 100S plasma sterilization (n=50) process. The results indicated minimal hole deformation from the ethanol and Sterrad sterilization processes but a complete collapse of holes in ETO-sterilized samples. As a result, the Sterrad 100S system was chosen as the sterilization method for our PLGA

conduits due to minimal degradation and deformation and verified sterility. This test is discussed in further detail in section 3.2.

An issue that resulted from the Sterrad sterilization process was the collapsing of conduit reservoirs on some devices. Due to the Sterrad process being processed under vacuum, as the system is reintroduced to atmospheric pressures, the pressure difference is enough to deform and permanently collapse the drug reservoirs. A final process of cutting a 2-3mm slit into the device wall was implemented to eliminate the collapsing of conduit reservoirs.

2.3. Device Verification Methodology: Release Kinetics

Verification tests were performed to ensure that the nerve conduits released drugs as expected. These *in vitro* tests were conducted by first loading each conduit reservoir with their respective drugs. For the tests specified above, they were loaded through the conduit slits that were cut to balance the reservoir pressures for reliable sterilization. Following loading, the devices are resealed using the same PLGA glue used during assembly. They are then attached to the side wall of their respective receiver chambers where tests are conducted. A 7mL transport tube was used as the receiver chamber for all of the tests conducted. PDMS was used to attach the devices to the wall in a location that would still allow for the devices to be fully submersed after the receiver chambers were filled with their test medium (either phosphate-buffered saline or growth media).

Once these tests were set up, samples were collected from the receiver chamber at determined time frames. Once the fluid was collected, the receiver chamber was flushed and new medium was added to the chamber. This simulated the body's natural ability to flush away drug once it was released from the devices. The *in vitro* tests were designed to

mimic the *in vivo* conditions of the conduits within the body. The flushing process of the receiver chamber imitates the body's natural process of fluid transfer around the implanted device which could be modeled as an instantaneous flushing of any drug leaked out of the device.

To prevent degradation, the samples were stored at -20°C for the dextran samples and -80°C for the NGF samples. Dextran samples were also stored in dark conditions to prevent fluorescent breakdown. Once enough samples were collected, they were loaded into 96 well plates and read using a fluorescent plate reader for dextran and corresponding enzyme-linked immunosorbent assay (ELISA) kits for NGF (rat betaNGF ELISA kit, Abcam). Each plate was loaded with a corresponding standard curve to correlate its fluorescence with a known concentration value.

The release data were processed by constructing a cumulative drug release over the entire test duration and plotted in correlation with the expected modelling results. Conversion between fluorescence values and concentration was done with a best fit using the standards for each plate. A percentage release was calculated by dividing the known released drug mass by the total drug injected into each device. Excel and MATLAB software was used to perform these calculations.

4 primary tests were performed:

1. An initial dextran release test using approximate zeroth-order release
2. A dextran release optimization test to release ~60% of the total drug over a 30-day interval
3. An NGF release test conducted in a simulated *in vivo* environment
4. A dextran release tests conducted in a simulated *in vivo* environment

2.3.1. Dual Conduit Zeroth-Order Release Test

The initial release test was conducted using dual mouse conduits in order to show that extended release was possible from the PLGA conduits. Initial tests were done with dextran, which is simpler and less expensive to measure, than the intended drugs. The dextran being released had two different fluorescent tags: Fluorescein (D1821, 10,000MW, Molecular Probes) and Texas Red (D1863, 10,000MW, Molecular Probes). These fluorescent dextrans were used because of their similar molecular weights and diffusion coefficients to one of the target drugs, NGF. These specific dextrans were chosen because their excitation and emission wavelengths occurred at different ranges (Fluorescein – Ex. 494 Em. 521; Texas Red – Ex. 595 Em. 615).

Along with verifying manufacturing techniques, this test was conducted with a 3% drug release over 30 days to demonstrate and measure steady chemical release. This design parameter was chosen to drive as close of a linear release as possible. By limiting the amount of active drug and increasing the starting concentration, the release model predicted a nearly zeroth-order release from these devices over 30 days.

This test was conducted using seven devices: Three devices with one 15 μ m diameter hole per drug reservoir (n=6) and four sealed devices that had no diffusion holes present. The sealed devices were used to verify assembly reliability. A negative control (device with no drug) was also used in the experiment. The drug reservoirs were approximately 20 μ L each and were loaded with a starting concentration of 50mg/mL of dextran. These tests were conducted at room temperature (~21°C) under nonsterile conditions. The devices were not sterilized before testing. Phosphate-buffered saline (PBS) was chosen as the receiver chamber medium and dilution fluid for all dextran testing.

2.3.2. Single-Conduit 60% over 30 Days Dextran Release Test

Following the results from the initial release test, additional refinement of delivery targets was determined. While releasing a constant delivery of drug from the conduit is the ideal, the bioactivity and efficacy of NGF on nerve cells spans a significant range. In order to more properly measure if the devices were releasing as expected, the release target was increased from a 3% release over 30 days to a 60% release over 30 days.

The conduits used to perform this test were designed to surgically reattach a rat's sciatic nerve and were constructed with a larger inner conduit than the mouse conduits. Single reservoir conduits were chosen for this test in order to minimize manufacturing variability and error. The drug reservoirs held approximately 20 μ L of drug and were loaded with an initial concentration of 10mg/mL of dextran (Fluorescein, D1821). The test was conducted using eight devices: six devices with one 130 μ m diameter hole and two sealed devices with no diffusion holes. A negative control with no drug was also used. These tests were conducted at room temperature (~21°C) under nonsterile conditions. The devices were not sterilized before testing.

2.3.3. Single Conduit NGF Release Test

The next level of progression with *in vitro* testing was simulating an *in vivo* environment. These devices were sterilized using the Sterrad 100S process and the diffusion tests were performed in an incubator at 37°C. The tests were performed using single reservoir rat conduits. Dextran was used through the previous tests due to its similar diffusion coefficient to NGF, but simulating actual NGF release is essential as proof of concept before *in vivo* testing.

This test was conducted using nine devices: three devices with one 130 μ m diameter

hole using a starting concentration of 0.025mg/mL NGF, three devices with one 130 μ m diameter hole using a starting concentration of 0.05mg/mL, and three sealed devices with no diffusion holes using a starting concentration of 0.05mg/mL. In addition to testing NGF release kinetics, two varying initial concentrations were tested to verify linear release scaling based on the amount of drug loaded. A negative control with no drug was also used.

These tests were conducted in an incubator (37°C) under sterile conditions. Device loading and sealing was done in a bio-sterile hood and the receiver chamber medium consisted of a media/fetal bovine serum (FBS) matrix containing growth media (DMEM F12, HyClone), 10% FBS (HyClone), and 1% antibiotic/antimycotic solution (HyClone). The NGF was diluted to the proper initial concentrations also using this media matrix. For *in vitro* testing, the range of delivery was selected based on the accurate range of the ELISA kits used to read the data.

2.3.4. Single Conduit Dextran Release Test at Simulated *in vivo* Conditions

Another dextran test was conducted to test the devices in sterile and incubation conditions. Dextran results are simpler to read and it is a cheaper alternative to NGF and also poses no risk of contamination, justifying performing additional tests with this approach. This test used the same 60% release target over 30 days as the previous dextran test. Single reservoir rat conduits were chosen for this test and they were sterilized using the 100S system. Fluorescein (D1821) was used as the release chemical and the receiver chambers were filled with 3mL PBS. The devices were loaded and tested under sterile conditions and the tests were conducted in an incubator (37°C). Eight devices were used for this test: five devices with 130 μ m holes were tested along with three sealed devices.

All the devices were loaded 20 μ L with an initial concentration of 5mg/mL. The tests were conducted out to 21 days.

2.4. Release Results and Discussion

2.4.1. Dual Conduit Zeroth-Order Release Test

Figure 2.4 shows the results from a 7-day collection. The release plot shows that the conduits were able to release drug consistently for an extended period of time. However, the sealed data also showed that it was hard to distinguish whether these devices were leaking from improper device sealing or if the drug was actually diffusing through the release holes, as the release from all conduits was above the predicted level. One important observation was that with each of these 7 devices, the reservoir assembly was successful in that 6 of the 7 reservoirs avoided mixing. This validated the construction and sealing techniques of the device.

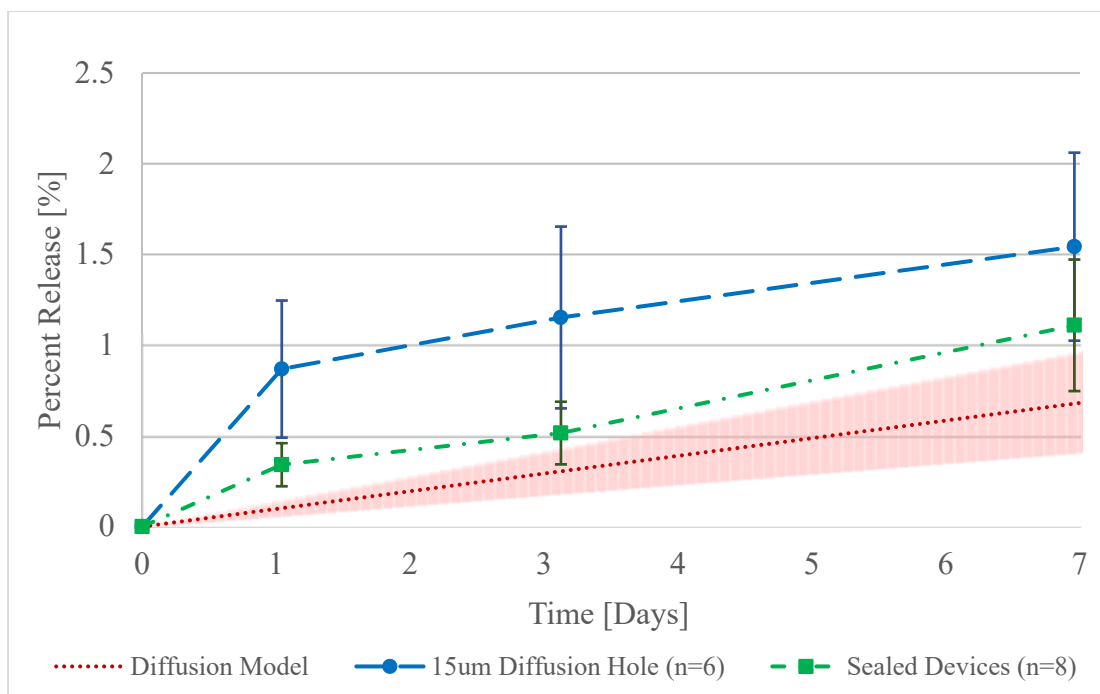


Figure 2.4: Zeroth-Order dextran release test using dual mouse conduits

2.4.2. Single-Conduit 60% over 30 Days Dextran Release Test

Figure 2.5 shows the results over a 43-day collection. The anticipated results from the diffusion model are shown in red with a $\pm 40\%$ error range shown. Further tests discussed later verified that this initial error range falls within the acceptable bioactivity levels where NGF has a positive effect on nerve growth. The results show two favorable conclusions: first, the sealed devices effectively released negligible material, verifying the construction of the conduit and adding confidence that the drug collected from the receiver chamber was actually being released through the diffusion holes in the inner conduit. Second, the 130 μm diffusion hole devices match very closely with the diffusion model over the entire collection period. The standard deviation of the six test devices fits within the 40% error range and conclusions can be drawn that under room temperature and unsterilized conditions, the nerve conduits deliver drug as expected.

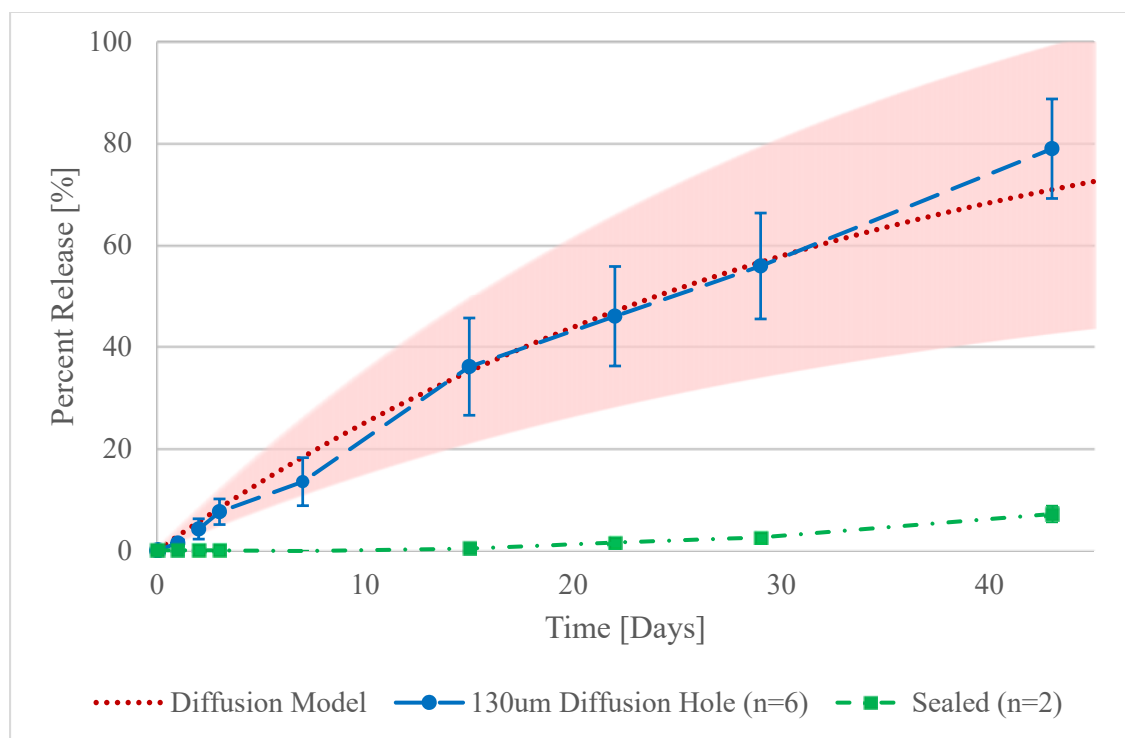


Figure 2.5: 60% dextran release test using single rat conduits

2.4.3. Single Conduit NGF Release Test

Figure 2.6 represents the data from the NGF release tests superimposed over its diffusion model. Neither of the test groups fell within the targeted range, but they were considerably higher than the sealed test group. However, all six devices released NGF at similar rates with little deviation, showing significant improvements in manufacturing reliability. This test was designed to release over a 30-day span, but the samples contaminated after 3 days and the test was conducted with PBS as the receiver medium after 8 days. A possible factor that may contribute to results that do not match release models is the acidity of the solution following contamination. NGF has been shown to have increased degradation under higher temperatures and lower pH levels [20]. While the exact mechanism for NGF degradation was not known, it is understood that between interaction with the contaminated sample and the change in acidity in the test chamber led to readings well below expectations.

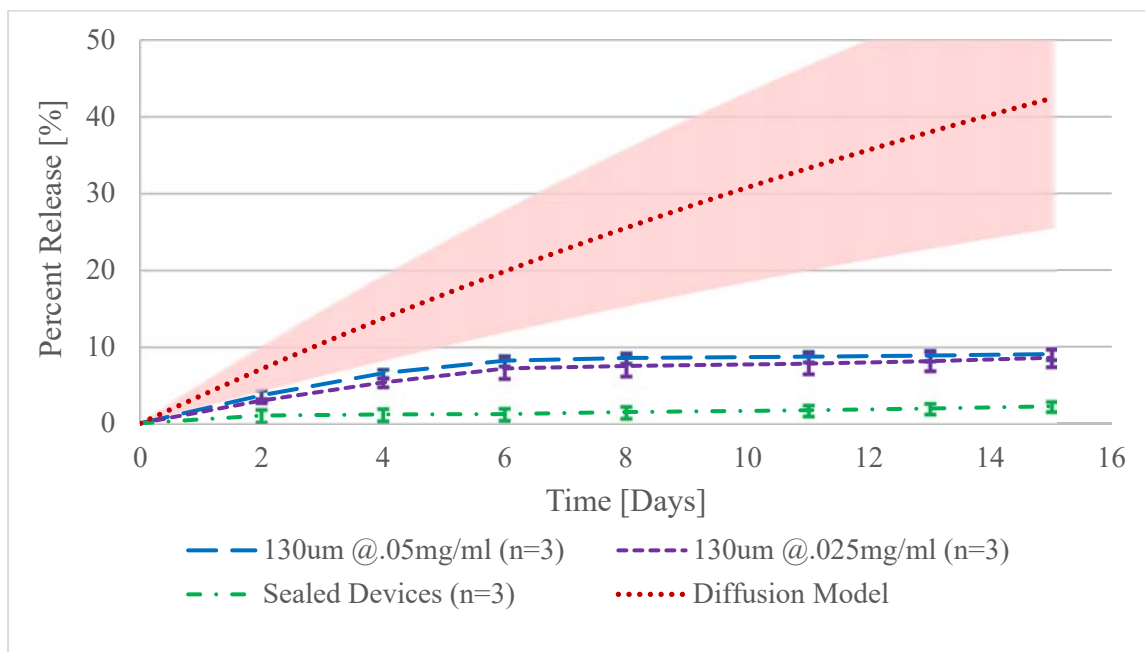


Figure 2.6: NGF release test conducted in *in vivo* environment

Even with the results likely altered due to contamination, there were still solid conclusions to be made from this test. Figure 2.7 shows the cumulative concentration release from the devices over time. In comparing the 0.025mg/mL and 0.05mg/mL starting concentrations of the two test groups, it is shown that the release from the 0.05 mg/mL devices closely resembles a doubling when compared to the 0.025mg/mL group. This verifies the ability to linearly scale the drug release range by varying the initial loaded concentration of drug. As a result, percent release can be viewed analogously to the actual amount of drug being released. This understanding is crucial in comparing drug release results between varying drugs because of different reading ranges for each of them. It is also important in being able to run optimized *in vitro* tests and then use those results to directly convert the results to an effective *in vivo* bioactive range.

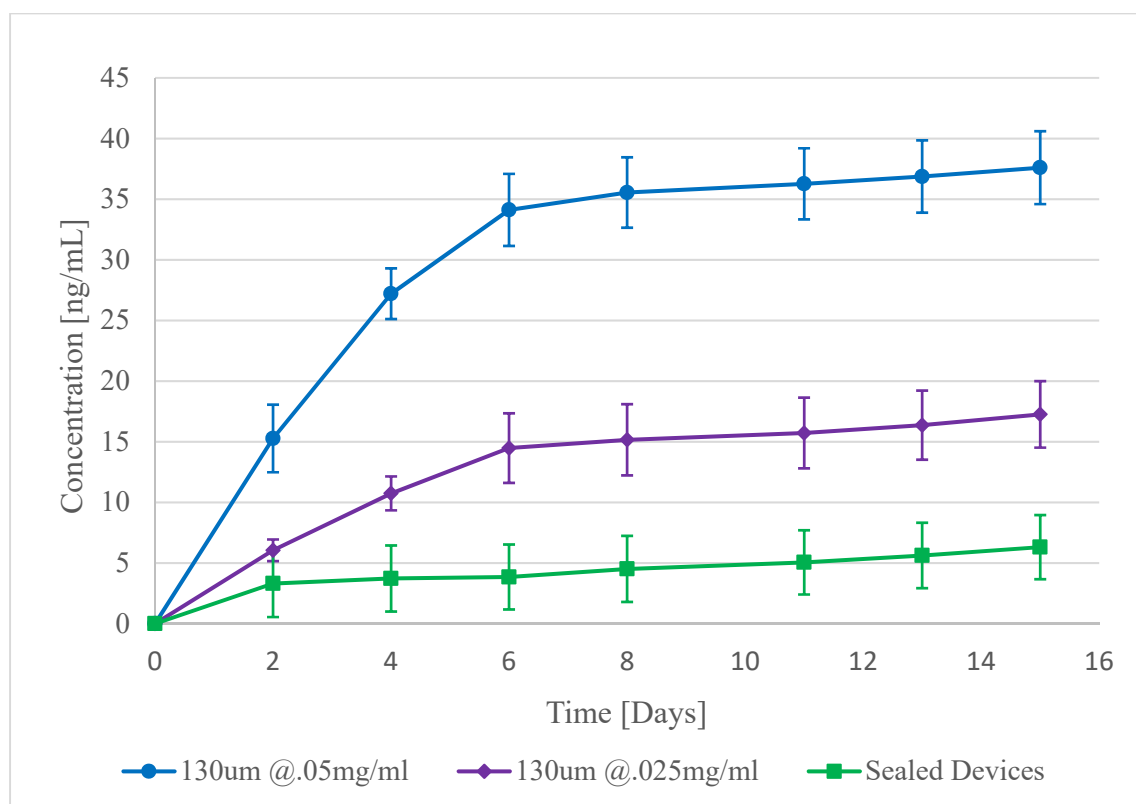


Figure 2.7: NGF cumulative concentration diffusion

One final observation from this test was increased polymer degradation from these contaminated devices. The PLGA devices that contaminated in this test swelled at a much quicker rate than devices that did not contaminate and also began disintegrating before the test was completed. It is still unknown whether the acidic conditions or the enzyme-rich environment played a larger role in this degradation, but it supports claims from other literature that degradation rate is affected by the PLGA solution environment. Actual degradation rates *in vitro* and *in vivo* do not align directly with PLGA's degradation due to hydrolysis and further tests must be performed to avoid problems with premature device degradation when *in vivo* tests are conducted in the future.

2.4.4. Single Conduit Dextran Release Test at Simulated *in vivo* Conditions

Figure 2.8 shows the results of the dextran release tests run in an incubator and sterile conditions. Drug release from the conduit appears to initially outpace the diffusion model and then slowly taper off after the first two days. It is to be noted that with the exception of one of the sealed devices that leaked and was considered an outlier, the results from both the sealed group and the diffusion hole group produced very small deviations. It is still unknown what is directly causing the variation in diffusion rate, but three hypotheses can be made. While the diffusion coefficient only changes by a small amount as the temperature is raised from 21°C to 37°C when it is placed in the incubator, the effects of temperature on the PLGA conduits is still unknown. It is possible that the swelling of the conduit material causes pressurization of the reservoirs and the initial drug burst is caused by that. Another hypothesis is that the diffusion holes were not completely stabilized, leading to a shrinkage of actual hole size and reduction in release rate.

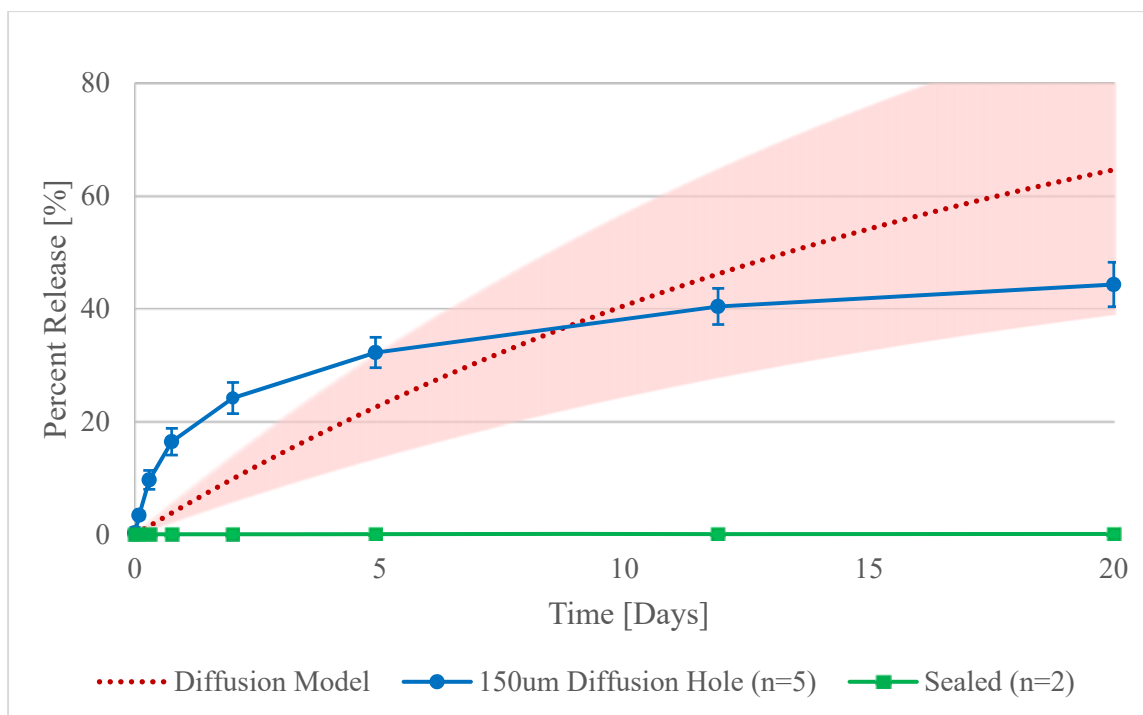


Figure 2.8: Dextran diffusion test conducted in *in vivo* environment

The final possible explanation can work in conjunction with the previous two. There are two main factors that can contribute to a different release rate in our conduits: release geometries and effective drug volume. While previous dextran tests at room temperature fell within our expected release rates, it is possible that at these elevated temperatures, some of the drug is becoming absorbed by the conduit and the amount of drug that is in the reservoir is reduced, providing a lower working volume. While it is seen that the diffusion rates do not match their ideals, the results still show promise by delivering a device that can still release drug within a bioactive range over 20 days. The factors that were affecting the drug release rates were universal, and additional tests would need to be conducted to isolate possible sources of variation.

CHAPTER 3

SUPPORT MATERIALS

This section is dedicated to materials that were support tests leading towards successful conduit diffusion. Many of the tests performed helped characterize PLGA and its untraditional mechanical behaviors that are negligible in many other engineering materials. PLGA is a fragile co-polymer that has very low melting point and even lower glass transition temperature (40-60°C). Consequently, a lot of processing techniques that are available for more stable materials are not an option for the polymer. Two tests that will be discussed involve the processing to produce diffusion holes that showed stability through the sterilization process as well as at *in vivo* conditions.

3.1. Diffusion Hole Stability

Results from Dextran tests ran at incubation temperatures showed a considerable drop-off in release after two days. It was assumed that the conduit diffusion holes were collapsing during that initial submersion period. PLGA is known to absorb water and can swell in size. Following testing results that showed variations to the diffusion models, several preliminary tests were conducted at 37°C and images were taken of the diffusion holes after certain time intervals. The device holes shrunk considerably after 24 hours (Figure 3.1). Following this initial swelling period, they appeared to stabilize. This indicates an explanation for the burst effect that is seen in the first day of drug delivery.

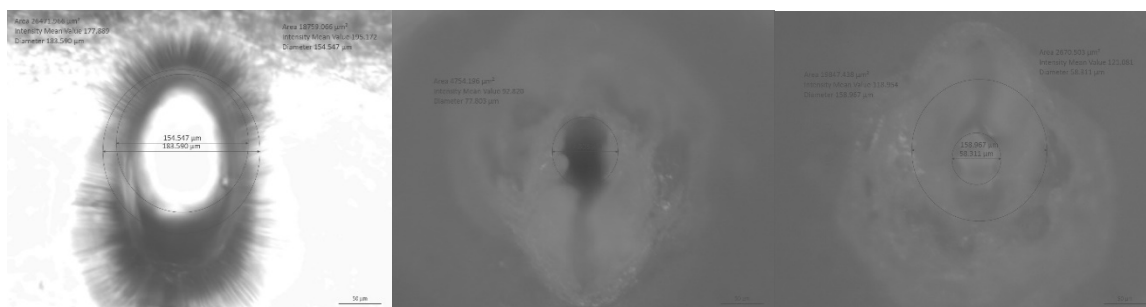


Figure 3.1: Diffusion hole shrinkage at 37°C a. after drilling (169 μm diameter) b. 24 hours after being submersed in PBS (78 μm diameter) c. 48 hours after being submersed in PBS (108 μm diameter)

Diffusion was chosen as the primary drug delivery mechanism due to its simplicity and predictability. PLGA's mechanical properties, like most polymers, can be modified through processing the material and modifying its crosslinking behavior. Since our holes are drilled using laser etching, it is possible that residual stresses build around the hole and the material does not get cut away. Instead, it recedes from the hole and as the conduit is placed back into incubation conditions and water, those stresses are relieved and the hole closes on itself.

As PLGA is exposed to elevated temperatures above its glass transition temperature, polymer chains form crosslinks. On a mechanical scale, that results in a much stiffer material. While the conduits as a whole need to maintain some level of suppleness in order to suture their ends and perform histology tests, overall drug diffusion seems to benefit from a more stable device. Local cross-linking at key areas such as the diffusion hole was hypothesized to stabilize diffusion results. A series of tests to stabilize the holes were performed on the holes including laser annealing, heat annealing, and plasma cross-linking. Lastly, a separate punching technique to form the holes was tested in lieu of laser etching.

3.1.1. Hole Processing

3.1.1.1. Laser Annealing

The laser annealing process involved using the laser cutter to locally heat the PLGA conduit around the diffusion hole. This was done by running multiple low-powered passes over the diffusion hole. When high power was used, the diffusion hole often became too big due to the residual heat but by running a low intensity 40x burst, the holes cut to similar geometries as desired. After these holes were drilled, the devices were submersed into water and placed in an incubator. Figure 3.2 shows images of these holes at time intervals of 0, 8, 24, and 72 hours after submersion. A total of 15 devices were tested using this procedure. Minimal shrinkage over this duration is observed.

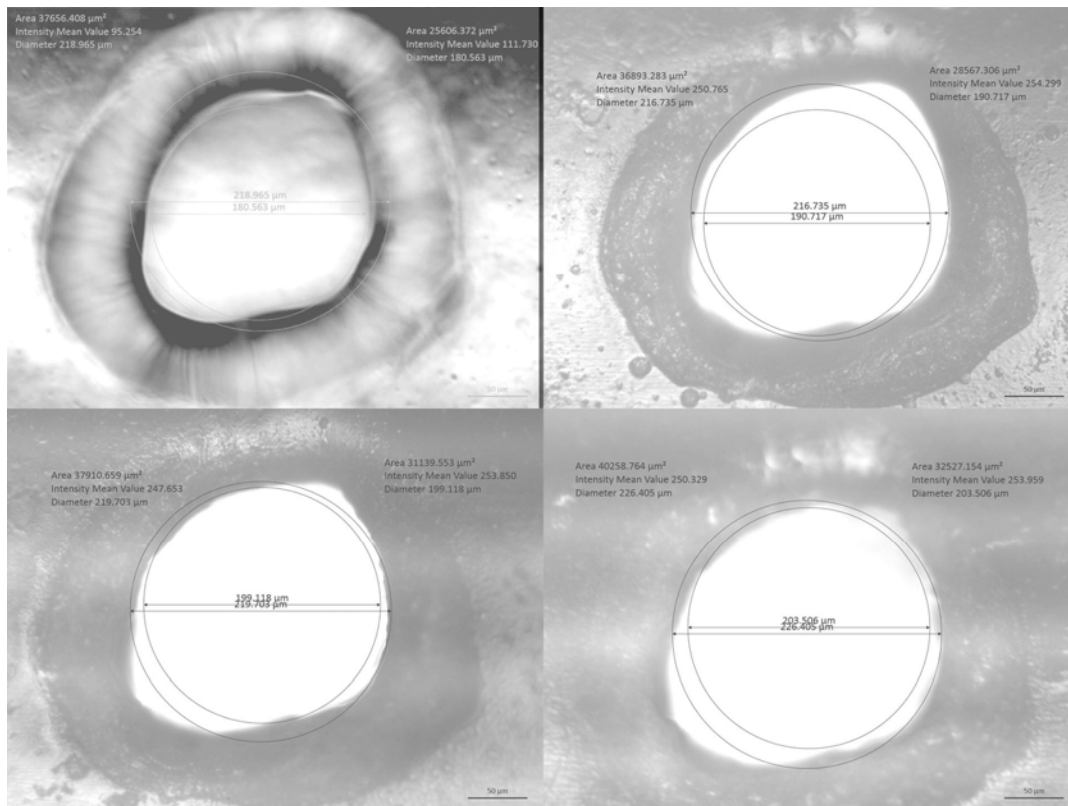


Figure 3.2: Laser-annealed hole after submersed in water at 37°C for a. 0 hours (200 μm) b. 8 hours (204 μm) c. 24 hours (210 μm) d. 72 hours (214 μm)

3.1.1.2. Heat Annealing

The heat annealing process was performed by taking a conduit with a previously drilled diffusion hole and heating it at 60°C for 30 minutes. In comparison to the laser annealing process, this treatment formed crosslinks within the entire conduit. It was unknown whether this would adversely affect the performance of the conduit so unless significant improvements were shown over the localized laser process, this process would be chosen as a secondary option. Following this, the conduit was tested for shrinkage. The devices were submersed into water and placed in an incubator. Figure 3.3 shows images of these holes at time intervals of 0, 8, 24, and 72 hours after submersion. A total of 2 devices were tested using this procedure. Minimal shrinkage over this duration is observed.

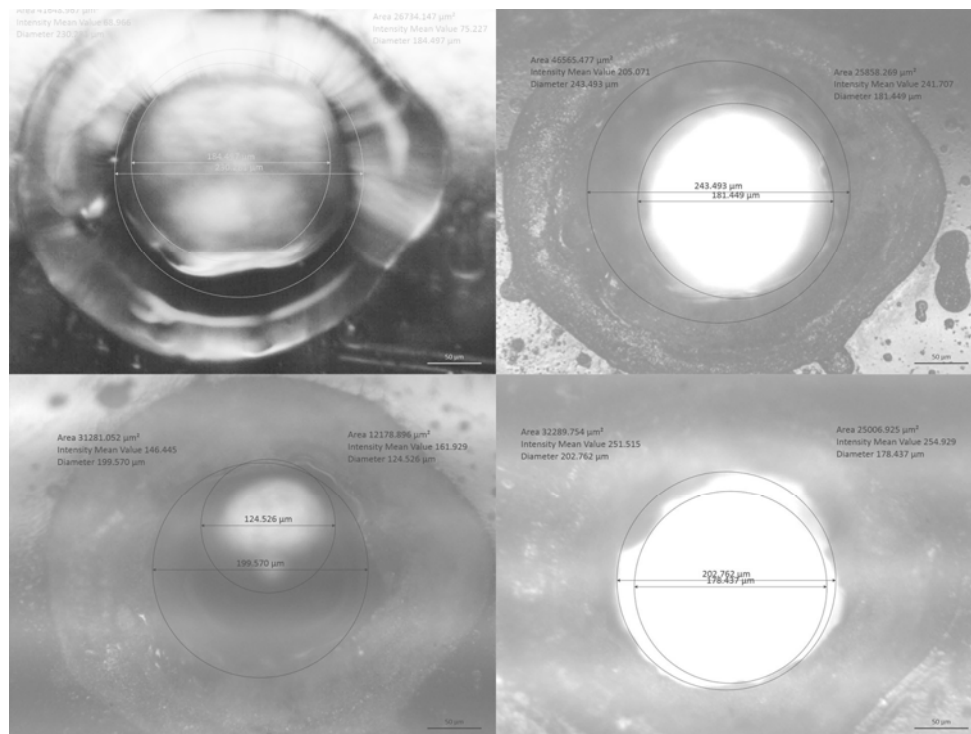


Figure 3.3: Heat-annealed hole after submersed in water at 37°C for a. 0 hours (207μm) b. 8 hours (212μm) c. 24 hours (162μm) d. 72 hours (191μm)

3.1.1.3. Plasma Crosslinking

The plasma crosslinking process was performed by taking a conduit with a previously drilled diffusion hole and exposing it to a corona plasma burst for 30 seconds. Plasma is known to break and rebuild crosslinks within polymers. By exposing the conduit to an extended plasma burst, these crosslinks would form at an accelerated rate and the rigidity of the polymer was expected to increase. The conduit was then tested for shrinkage. The devices were submersed into water and placed in an incubator. Figure 3.4 shows images of these holes at time intervals of 0, 8, 24, and 72 hours after submersion. A total of 2 devices were tested using this procedure. Minimal shrinkage over this duration is observed.

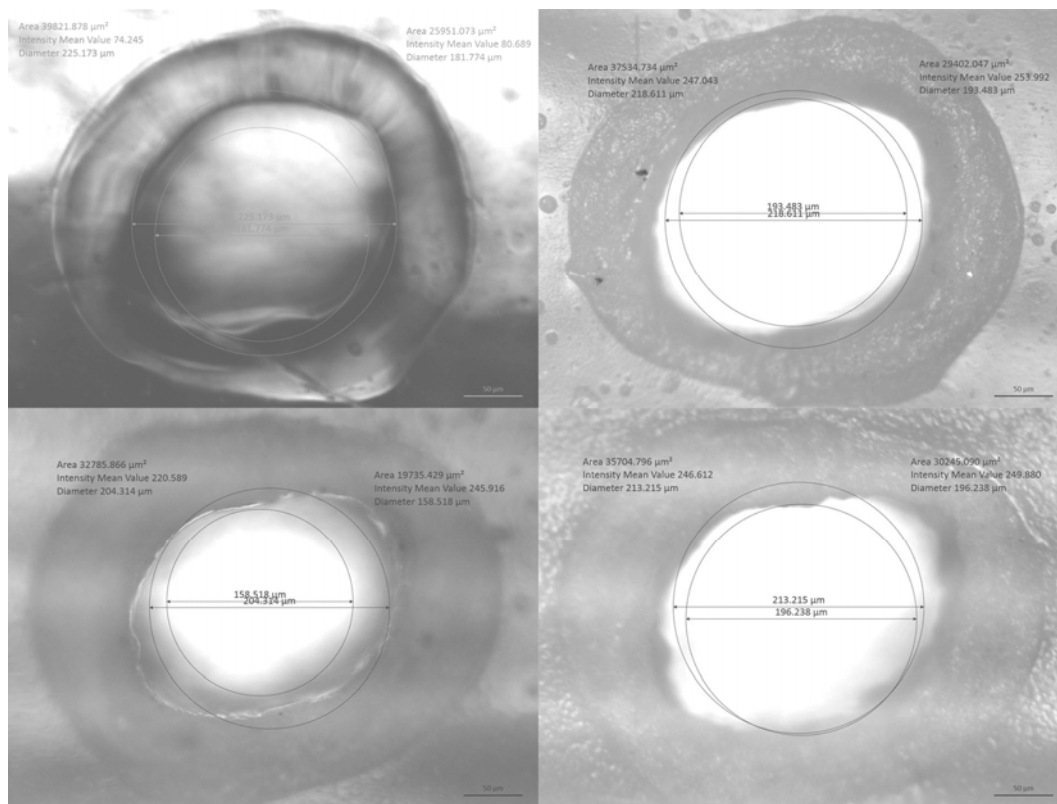


Figure 3.4: Plasma-processed hole after submersed in water at 37°C for a. 0 hours (204 μm) b. 8 hours (206 μm) c. 24 hours (182 μm) d. 72 hours (205 μm)

3.1.1.4. Hole Punching

It is assumed that the diffusion holes shrunk so aggressively because no material is actually removed during the laser drilling process. Instead, it melts away from the drill site and the residual stresses force the hole shut as the conduit is placed into testing conditions. Instead of using a laser to drill the diffusion holes, a 30-gage wire was sharpened and used to punch a diffusion hole. The dimensions of a 30-gage wire are .159mm ID and .311mm OD. The conduit was then tested for shrinkage. The devices were submersed into water and placed in an incubator. Figure 3.5 shows images of these holes at time intervals of 0, 8, 24, and 72 hours after submersion. One device was tested using this procedure. After 8 hours, the hole appears to shrink considerably (from 244 μ m to 131 μ m) but the hole maintains its geometry afterwards.

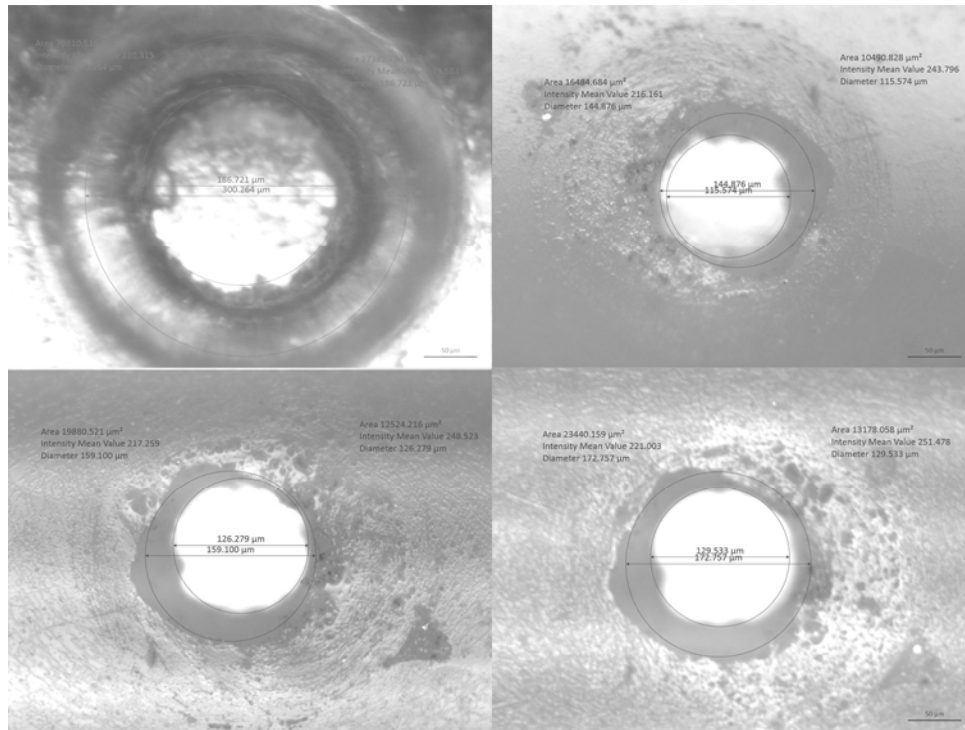


Figure 3.5: Punched hole after submersed in water at 37°C for a. 0 hours (244 μ m) b. 8 hours (131 μ m) c. 24 hours (143 μ m) d. 72 hours (152 μ m)

3.1.2. Hole Stabilization Conclusions

The results from these tests show that all of the processing techniques yield more favorable results than unprocessed conduits. Both annealing processes and the plasma cross-linking process seemed to prevent the holes from shrinking or swelling as they did when unprocessed. The punched hole appears to show the effect of both a cored and stretched hole during the punching process. Initially, the hole resembles a diameter closer to that of the punch outer diameter. After the conduit was submersed for 8 hours, the region that could have been stretched out over the punch taper appears to swell back and the hole shrinks down to a size comparable to the punch inner diameter. While no additional tests were performed with this manufacturing method because it would be harder to perform than the other methods tested on a large scale, it proves to be a viable backup method and produces more circular holes than laser drilling. Laser annealing was chosen as the hole processing method mostly because it only alters the material on a localized area near the hole instead of over the entire inner conduit.

3.2. Sterilization

PLGA poses a few problems regarding sterilization. It is a reactive polymer that may break down from certain radiation or chemical sterilization processes. Because PLGA has a relatively low glass transition temperature, many traditional sterilization methods like autoclaving are not an option. Previously, our devices showed considerable shrinkage when sterilizing devices, leading to inconsistencies in diffusion properties caused by varying drug reservoir volumes as well as changing diffusion hole sizes. Some sterilization techniques also have significantly changed our materials and lead to hardened devices and degradation in the polymeric structure. This poses a problem when

implanting the devices, making them hard to manipulate and suture into place.

Previous literature suggested that three sterilization methods produced more stable and repeatable results with 85/15 PLGA: plasma sterilization, ethylene oxide (ETO), and ethanol [19]. Their tests indicated that plasma set at 100% power typically shrunk PLGA by up to 50%. However, plasma set at 50% power had no effect on geometric integrity. ETO was found to shrink PLGA by ~60% and also reduced its molecular weight significantly from polymer degradation. When soaking PLGA in 70% ethanol, their tests indicated no significant geometric effects or polymer degradation; however, the biocompatibility tests revealed poor sterilization results. The goal in the following sterilization tests was to determine the best technique to produce repeatable sterilized conduit devices while limiting PLGA degradation and preserving the mechanical integrity of the conduits.

The following methods were tested for sterilization:

- Sterrad Plasma Sterilization (ASP Sterrad 100S System): (50% power)
- Ethylene Oxide
- 70% Ethanol: PLGA conduits were soaked in ethanol for 30 minutes and then promptly removed. Following this, they were bathed in water for 6 hours to displace the solvent and re-harden the polymer.

Each test used four conduits ($n=4$) with each one containing eight diffusion holes (~120-150 μm diameter). These holes were drilled using a laser and each one had a small inward taper of $\sim 10^\circ$ from the residual laser energy. Two of the conduits were sterilized while fixed on a needle to retain cylindrical structure while the other two were sterilized freely without structural backing.

3.2.1. Sterrad

For these devices, the holes (n=36) remained approximately the same size (<20% change). This was in contrast to our sterilization results using a Sterrad 100NX procedure at 90% power. Under those test conditions, the PLGA conduits shrunk and deformed by up to 50% volume. For the Sterrad 100S system at 50% power, the conduits maintained their geometric integrity (Figure 3.6). They also retained a similar hardness to their presterilization conditions. This was important for preserving the ability to suture the conduits to the nerve endings.

3.2.2. Ethylene Oxide

Following ETO sterilization, all of the devices significantly deformed from their original cylindrical shapes and all of the diffusion holes fused (Figure 3.7). Each conduit also significantly hardened from the process. The PLGA conduits are highly sensitive to temperature and the ETO process is run at 60°C. However, the chemical sensitivity of the polymer to the ETO process is unknown. Regardless, from these observations, it was concluded that the ETO process we used was too aggressive and unstable for 75/25 PLGA conduits.

3.2.3. Ethanol

The conduits sterilized with ethanol were slightly larger poststerilization and the diffusion holes expanded slightly (~25%) at their bottom tapers (Figure 3.8). However, a major consideration for avoiding this process is because of its nontraditional nature. It would be hard to show the sterilization justification of these conduits. In addition, there would be extensive training required to ensure that the sterilization procedure was done properly, compared to the standard procedures that Sterrad and ETO sterilization offer.

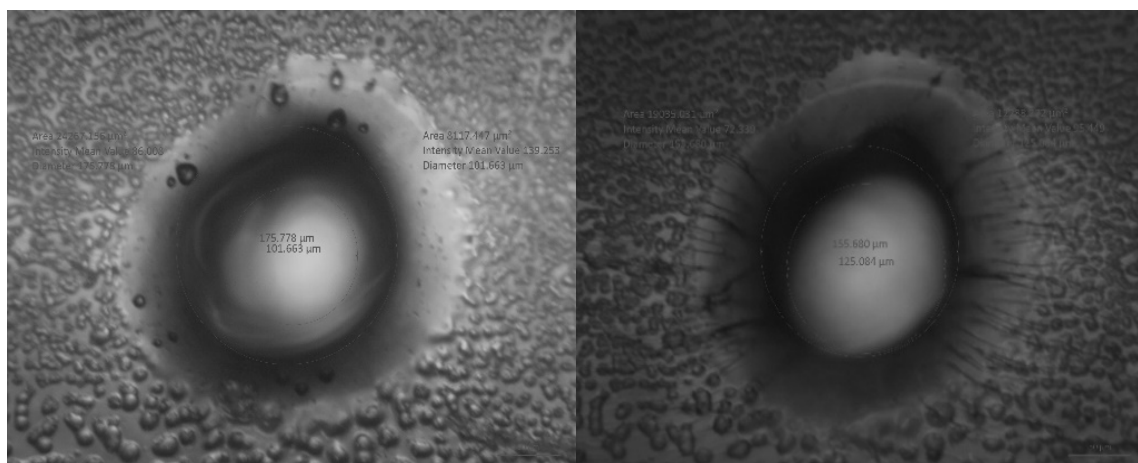


Figure 3.6: Sterrad presterilization hole (176/102 μm , left) and poststerilization hole (156/125 μm , right)

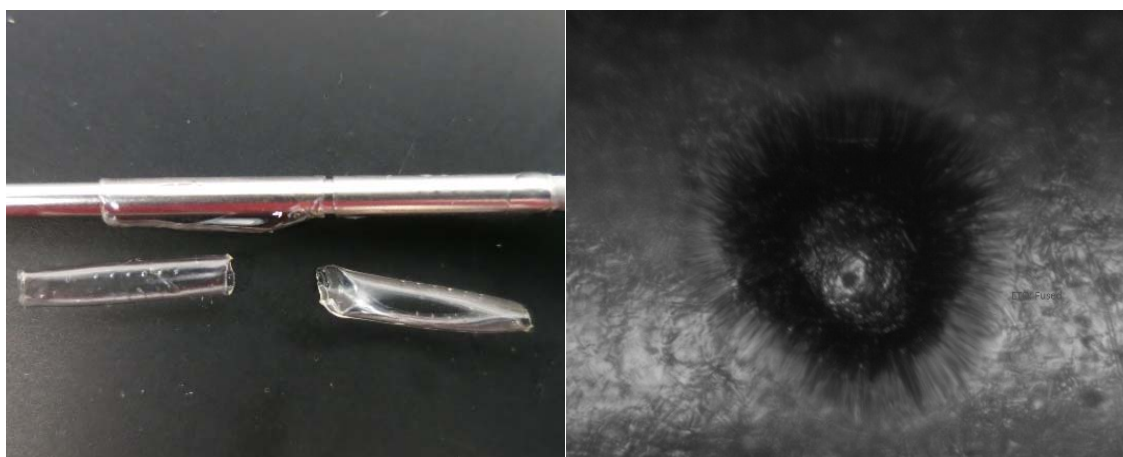


Figure 3.7: Ethylene oxide poststerilization deformation (left) and sealed hole (right)

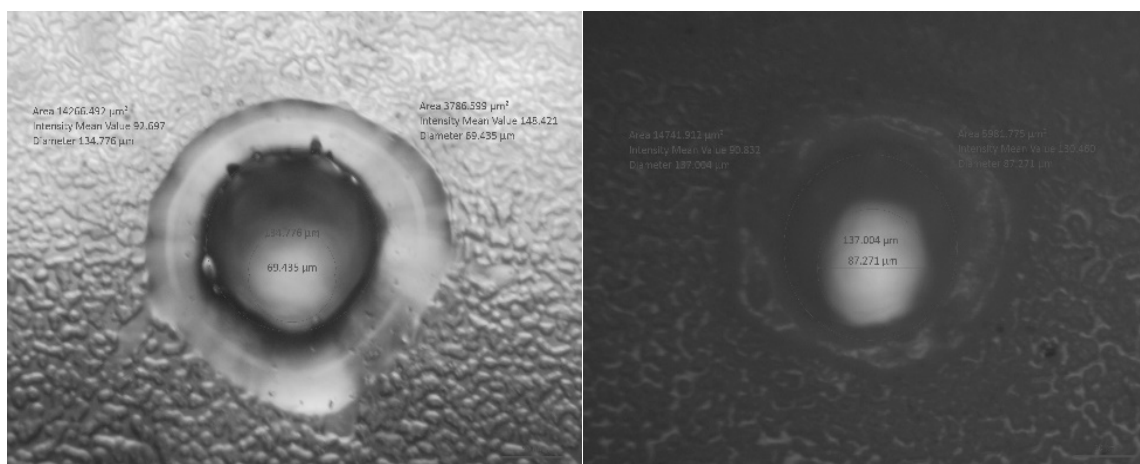


Figure 3.8: Ethanol presterilization hole (135/69 μm , left) and poststerilization hole (137/87 μm , right)

3.2.4. Sterilization Justification

Based on the results of these tests, Sterrad sterilization using the 100S system at 50% power minimized negative effects on the diffusion holes. Degradation, shrinkage, and deformity caused by ETO sterilization eliminate its viability for PLGA conduits. Ethanol sterilization is a viable option regarding polymeric degradation and geometric consistency but it is unknown whether this method can sufficiently sterilize the devices for implantation. Because there is little deformation caused by the Sterrad system, holes can consistently be drilled and diffusion tests will have more reliability than the other sterilization methods.

One final issue that resulted from the Sterrad sterilization process was the collapsing of conduit reservoirs. It is theorized that due to the Sterrad process being processed under vacuum, as the system is reintroduced to atmospheric pressures, the pressure difference is enough to deform and permanently collapse the drug reservoirs. In order to avoid this, a final process of cutting a slit into the device wall was implemented to eliminate the collapsing of conduit reservoirs.

CHAPTER 4

CONCLUSIONS

The results of the *in vitro* drug release tests offer positive insight into the reliability and function of our nerve conduits. The following section includes conclusions and contributions that were made through the course of this project and also explores future direction for the project.

4.1. Conclusions

This project started in continuation to previous work on nerve conduits. The goal of successfully facilitating nerve regeneration through a guidance conduit was further developed. A revised diffusion model was generated to predict diffusion rate based on critical variables. The PLGA manufacturing process was refined to produce more consistent conduits. These bioresorbable conduits were tested to verify diffusion by running bench tests and comparing drug release results to numerical models.

The first of these tests was conducted at room temperature with dextran release drug and verified that sustained drug release was possible. The second diffusion test worked from the first test's results and it was decided that increasing the target diffusion rate would result in more consistent drug release and minimize error. This test was also performed at room temperature with nonsterilized devices. The results verified consistent release very close to the predicted values. A third diffusion test was conducted to test a

bioactive release of NGF from the devices as well as sterilized devices at body temperature. This test resulted in contaminated samples and a revised protocol was developed to eliminate this risk in future bench tests. However, functional data were produced from this test. The sealed devices maintained their integrity and results showed a linear relationship between starting concentration and drug released. The final test was conducted using dextran release and the tests were performed at *in vivo* conditions (sterile, body temperature). While the drug diffusion followed a different release rate than expected, they still remained in the bioactive range and the release data produced the smallest standard deviations to date. Further investigation is required to determine the cause of increased initial drug burst but possible causes include pressurized devices due to PLGA shrinkage. Additionally, a reduced hole size from the polymer swelling could have reduced the diffusion over time.

4.1.1. Drug Release

- Diffusion of drug through our conduits can be tuned by both linear scaling and diffusion rate.
 - Diffusion rate is dependent on the hole size, reservoir size, wall thickness, and other conduit geometries.
 - Linear scaling can be achieved by modifying the initial concentration of drug loaded.
- Multireservoir conduits can be fabricated and drug can be released over a 30-day span.
- At room temperature conditions, kinetics from the devices fell within the bioactive range of drug released.

- Drug release rates are independent of loading concentrations; consequently, actual dosage rates can be linearly scaled to any level.

4.1.2. Device Structure

- In situations where contamination was present, PLGA devices degraded at an accelerated rate
 - This suggests that hydrolysis is accelerated in these conditions or there are other mechanisms leading to the polymer degradation outside of hydrolysis
- Sterilization of the PLGA conduits can be achieved using a Sterrad plasma system, yielding sterile devices that maintain their structural integrity.
- PLGA naturally swells when exposed to water for extended periods and additional processing must be performed to prevent geometric deformations.
 - Diffusion holes in PLGA can shrink when placed in water at elevated temperatures

4.2. Contributions

4.2.1. Modelling

- Developed release model that can predict the drug release rate from our nerve conduits for any reservoir size, diffusion hole size, initial drug concentration, conduit size or geometry, number of drug reservoirs, or drug diffusion coefficient. The models can accommodate time-dependent geometric variances as well.
- Developed correlation models between *in vitro* collection concentrations and the concentration gradient of drug within the inner conduit that depicts the instantaneous concentration that cells react with *in vivo*.

4.2.2. PLGA Processing and Manufacturing

- Developed system to track individual devices through their manufacturing process in batches up to 50 devices.
- Constructed jig fixture to aid with assembly of devices and drug loading.
- Developed solvent welding techniques to seal PLGA devices.
- Developed and optimized diffusion hole stabilization techniques.
- Determined proper techniques to prevent reservoir collapse during the Sterrad sterilization process.
- Developed drug loading techniques to fill and seal drug reservoirs

4.2.3. Release Kinetics

- Developed proper sterile condition protocols for loading and collecting *in vitro* test samples.
- Developed postprocessing techniques to convert fluorescent readings into concentration values for Dextran and NGF.
- Optimized *in vitro* collection protocol to minimize disruption in diffusion.

4.3. Future Work

Future work on this project will include completion of *in vivo* tests that show proper functional recovery on sciatic nerve lesions in mice and rat implantations. The first of these studies will be performed using a comparison of autografts (n=16), nerve conduits loaded with NGF (n=16), and nerve conduits without any drug delivery (n=16).

These animal tests will be essential to validating device performance in bodily conditions. Functional recovery is the ultimate goal of the nerve conduits and walking

tracks and comparison to autologous grafts will serve as a benchmark to determine the efficacy of the device. In addition, histological tests will be used to observe the growth patterns of the nerve endings through the guidance conduit. The integrity of the conduit is essential to extended drug diffusion and an *in vivo* test will determine if the PLGA devices can withstand the environmental forces as well as the fluidic and enzyme conditions found in a body.

The latter half of testing through this thesis was done using single rat conduits; comparable results will have to be generated using dual release mouse conduits. Such work will require miniaturization of the devices. The duration of diffusion is controlled by two factors: diffusion rate and total amount of drug available. As the drug volume shrinks, a slower diffusion rate is required to prolong diffusion over an equivalent time period. As a result, diffusion hole drilling techniques that result in more stable holes will have to be developed and optimized.

Another problem that we encountered during testing at elevated temperatures is instability of PLGA. Further tests to reinforce the bulk structure and the diffusion holes will be conducted, but if they cannot be stabilized, the advantages of a diffusion release will be negated and alternative materials will have to be explored. Some materials that we know retain longer half-lives and could potentially withstand *in vivo* conditions include PGA and collagen. In parallel to this research, it would be valuable to conduct tests with nondegradable devices that are known to maintain their structural stability to further confirm the diffusion models and design of the drug release conduit while avoiding issues with PLGA. Once the diffusion models and tests are confirmed and optimized, material behavior of untraditional degradable materials can be benchmarked against those

standards.

The tests discussed above will provide more concrete data on the performance of the devices. Building a nondegradable device will ensure the design is functional and will allow us to optimize the diffusion model and its constants. There are additional polymer-stabilizing processes that still need to be tested to determine if PLGA is a viable diffusion conduit material. If it proves too difficult to produce devices that perform as desired in the body, other more stable degradable materials such as PGA or collagen can be tested. These additional studies will drive forward the development of a successful drug delivery nerve guidance conduit to provide a viable option for peripheral nerve regeneration.

APPENDIX

DIFFUSION MODEL – MATLAB CODE

Fick's Diffusion Function

The following code is the function that depicts calculations performed for the Fick's

Diffusion model.

```
%  
% Ficks_Diffusion.m  
%  
% Scott Ho  
% Created: 5/8/14  
%  
% Function to perform diffusion calculations according to Fick's Law  
% Multistep function: 3 steps (reservoir, hole, conduit, receiver  
% chamber)  
%  
% Inputs:  
%     Select proper model [model_select, 0 (receiver) or 1 (stump)]  
%     Diffusion coefficient [D_coeff, cm^2/s]  
%     Reservoir initial concentration [C_reservoir, mg/ml]  
%     Thickness of inner conduit [t_IC, mm]  
%     Length of inner conduit [L_IC, mm]  
%     Initial and final times [time_i, time_f, hr]  
%     Number of iterations [iterations, integer]  
%     Collection times [collections, days]  
%     Reservoir volume [V_reservoir, ml]  
%     Diffusion Hole diameter [diam_hole, um]  
%     Number of Diffusion Holes [hole_count, integer]  
%     Inner Conduit diameter [diam_IC, mm]  
%     Receiver Chamber Volume [V_receiver, ml]  
%     Length of nerve stump [L_stump, mm]  
% Outputs:  
%     Array of total concentration over time [C_out_all, ng/ml]  
%     Receiver concentration values at collection times  
[C_out_collections, mg/ml]  
%     Time at collection [t_collections, sec]  
%     Instantaneous concentration at the diffusion hole exit  
[C_conduit, mg/ml]  
%     Instantaneous drug mass at the diffusion hole exit [M_conduit,  
mg]  
%     Array of total mass exit over time [M_out_all, mg]
```

```

% Assumptions made for the following model: linear diffusion, steady-
state
% (no velocity gradient), D taken from literature, neglecting edge
effects
% and PLGA interaction, well-mixed homogeneous fluid.
%
%
% Receiver chamber - model_select is 0
% Nerve Stump/In-vivo - model_select is 1
%
% Receiver chamber model: Concentrations at the receiver chamber are
summed
% together and continue to collect until the chamber is flushed
%
% Stump model: Inner conduit instantaneous concentration gradient is
% outputted and correlated to the equivalent amount of drug diffused
from
% the conduit

function [C_out_all, C_out_collections, C_cumulative, t_collections,
C_conduit,...
    M_conduit, M_out_all] = Ficks_Diffusion(model_select, D_coeff,...
    C_reservoir, t_IC, L_IC, time_i, time_f, iterations,
collections,...
    V_reservoir, diam_hole, hole_count, diam_IC, V_receiver, L_stump)

%%% Unit Conversions to standard units, model parameter, and
dimensional
%%% values for calculation
concentration = C_reservoir; %mg/ml
mass_reservoir = concentration*V_reservoir; %mg
%Set diffusion lengths according to device and setup geometries
L12 = t_IC/10; %convert mm to cm
if model_select == 0
    L23 = L_IC/2/10; %convert mm to cm
    L34 = 0;
else
    L23 = (L_IC/2 - L_stump)/10; %convert mm to cm
    L34 = (L_stump)/10; %convert mm to cm
end
time_i = time_i * 60*60; %convert hrs to sec
time_f = time_f * 60*60; %convert hrs to sec
time = linspace(time_i, time_f, iterations); %time array in sec
delta_t = time(2)-time(1);
%map collection times to their proper iteration times in seconds
for map = 1:size(collections,2)
    collections(map) = collections(map)*24*60*60; %convert days to
seconds
    [~, index] = min(abs(time-collections(map)));
    collections(map) = time(index);
end

diam_hole = diam_hole*1e-4; %convert um to cm
diam_IC = diam_IC/10; %convert mm to cm
A12 = pi*(diam_hole/2)^2*hole_count;%cm^2
A23 = pi*(diam_IC/2)^2; %cm^2

```

```

V1 = V_reservoir; %cm^3,ml
% V12 = A12*t_IC; %cm^3,ml
% V23 = A23*L23; %cm^3,ml
V3 = V_receiver; %cm^3,ml
% V34 = A34*L34; %cm^3,ml
%%%
%%%

%initialize concentration/mass and flux arrays
M1 = mass_reservoir*ones(size(time));
M2 = zeros(size(time));
M3 = zeros(size(time));
M_out_all = zeros(size(time));
M_out_collections = zeros(size(collections));
JM1 = zeros(size(time));
JM2 = zeros(size(time));
C1 = concentration*ones(size(time));
C2 = zeros(size(time));
C3 = zeros(size(time));
C_out_all = zeros(size(time));
C_out_collections = zeros(size(collections));
C_cumulative = zeros(size(collections));
J1 = zeros(size(time));
J2 = zeros(size(time));

t_collections = zeros(size(collections));
collection_count = 1;

%Loop through time iterations
for step = 1:size(time,2)

    %%%%%%%%%code for receiver chamber model%%%%%%%%%
    if model_select == 0
        % syms conc1 conc2 conc3
        % C2_eq(conc1,conc3) = solve(-D_coeff*(conc1-conc2)/L12*A12 ==
        -D_coeff*(conc2-conc3)/L23*A23, conc2);
        % C2(step) = C2_eq(C1(step),C3(step));
        %simplified C2 equation
        C2(step) = (A12*L23*C1(step) + A23*L12*C3(step))/(A12*L23 +
A23*L12);
        M2(step) = (A12*L23*M1(step) + A23*L12*M3(step))/(A12*L23 +
A23*L12);
        J1(step) = -D_coeff*(C1(step)-C2(step))/L12;
        JM1(step) = -D_coeff*(M1(step)-M2(step))/L12;
        J2(step) = -D_coeff*(C2(step)-C3(step))/L23;
        JM2(step) = -D_coeff*(M2(step)-M3(step))/L23;

        %Flush check: if receiver chamber is sunk, reset receiver
        %concentration to 0. Models flushing of samples.
        for count = 1:size(collections,2)
            if collections(count) == time(step)
                %output receiver chamber concentration at collection
times

                C_out_collections(collection_count) = C3(step);
                M_out_collections(collection_count) = M3(step);
                t_collections(collection_count) = time(step);
            end
        end
    end
end

```

```

        collection_count = collection_count + 1;
        C3(step) = 0;
        M3(step) = 0;
    end
end

C1(step+1) = C1(step) + J1(step)*A12*delta_t/V1;
M1(step+1) = M1(step) + JM1(step)*A12*delta_t/V1;
C3(step+1) = C3(step) - J2(step)*A23*delta_t/V3;
M3(step+1) = M3(step) - JM2(step)*A23*delta_t/V3;

% output concentration/mass at the exit of the diffusion
hole(s), J2
    C_conduit = C2(step);
    M_conduit = M2(step);
    % output receiver chamber concentration in mg/ml
    C_out_all(step) = C3(step);
    M_out_all(step) = mass_reservoir - M1(step);
    % cumulative concentration for flushed samples
    C_cumulative(step) = C_out_all(step) + sum(C_out_collections);
    %%%%%%%%%%%%%%%%%%%%%%%%%%%%%%%%%%%%%%%%%%%%%%%%%%%%%%%%%%%%%%%%%%%%%%%%%

    %%%%%%%%%code for nerve stump in-vivo model%%%%%%%%
    else
        %      syms conc1 conc2 conc3
        %      C2_eq(conc1,conc3) = solve(-D_coeff*(conc1-conc2)/L12*A12 ==
        %      -D_coeff*(conc2-conc3)/L23*A23, conc2);
        %      C2(step) = C2_eq(C1(step),C3(step));
        %simplified C2 equation
        C2(step) = (A12*L23*C1(step) + A23*L12*C3(step))/(A12*L23 +
A23*L12);
        M2(step) = (A12*L23*M1(step) + A23*L12*M3(step))/(A12*L23 +
A23*L12);
        J1(step) = -D_coeff*(C1(step)-C2(step))/L12;
        JM1(step) = -D_coeff*(M1(step)-M2(step))/L12;
        J2(step) = -D_coeff*(C2(step)-C3(step))/L23;
        JM2(step) = -D_coeff*(M2(step)-M3(step))/L23;
        C1(step+1) = C1(step) + J1(step)*A12*delta_t/V1;
        M1(step+1) = M1(step) + JM1(step)*A12*delta_t/V1;

        %Output conduit concentration at 'collection' times
        for count = 1:size(collections,2)
            if collections(count) == time(step)
                %output receiver chamber concentration at collection
times
                    C_out_collections(collection_count) = C2(step);
                    M_out_collections(collection_count) = M2(step);
                    t_collections(collection_count) = time(step);
                    collection_count = collection_count + 1;
            end
        end

        % output internal steady-state concentration/mass at the exit
of
        % diffusion hole

```

```

        C_conduit(step) = C2(step);
        M_conduit(step) = M2(step);
        % output total drug diffused concentration in mg/ml; ignore
first
    % point
    if step ~=1
        C_out_all(step) = C_out_all(step-1) + C_conduit(step);
        M_out_all(step) = mass_reservoir - M1(step);
    end
    %%%%%%%%%%%%%%%%%%%%%%%%%%%%%%%%%%%%%%%%%%%%%%%%%%%%%%%%%%%%%%%%%%%%%%%%%
end
end
end

```

In vitro Release Parameters

The following code is the script that takes input parameters for the nerve conduit, runs the diffusion model, and outputs collection concentrations and plots over time for *in vitro* modelling.

```

%
% Diffusion_NGF_receiver.m
%
% Scott Ho
% Created: 5/8/14
%
% Diffusion Modelling: Model used to determine proper hole sizes and
% expected diffusion rate for receiver chamber
%

%% NGF/Dextran Parameters

% NGF/Dextran: molecule size chosen by matching diffusion coefficient
with NGF
% coefficient.

%%%%%%%%%%%% Input Parameters: NGF/Dextran + Rat Single
Conduit %%%%%%%%%%%%%
conc_reservoir = 5;          %mg/ml
%time of tests in days
time_i = 0;
time_f = 30;
time_i_hr = time_i*24;
time_f_hr = time_f*24;
%number of iterations: over 200 iterations should be accurate to
within .1%
%cumulative diffusion; for under 1% collection error, use 400+
%iterations
iterations = (time_f_hr-time_i_hr)*2;
collections = [time_i 1 2 4 7 14 21 28 time_f];    %in days
no_collect = 0;
D_coeff_ngf = 1.26e-6;    %cm^2/sec

```



```

%hole parameters
hole_diam = 130;          %um
hole_count = 1;

%Rat Single Conduit size
%length of reservoir: dual conduit
res_length = 7;          %mm
% prompt1 = 'Length of Drug Reservoir (mm)?\n';
% res_length = input(prompt1);
%reservoir outer diameter: determined by outer conduit ID
res_OD = 3.0;            %mm
length_IC = 13;          %mm
receiver_volume = 3;      %ml
%Stump not used in receiver chamber tests; make dummy variable
stump_length = 0;        %mm
%reservoir inner diameter: determined by inner conduit OD
res_ID = 2.3;            %mm
%reservoir volume
reservoir_volume = res_length*pi*((res_OD/2)^2-(res_ID/2)^2); %ul
fprintf('Reservoir Volume: %.1f ul \n\n', reservoir_volume)
reservoir_volume = reservoir_volume*.001; %ul to
ml

%conduit inner diameter: matches 14G needle OD
conduit_ID = 2.01;       %mm
thickness_IC = (res_ID-conduit_ID)/2; %mm
%%%%%%%%%%%%%%%%%%%%%%%%%%%%%%%%%%%%%%%%%%%%%%%%%%%%%%%%%%%%%%%%%%%%%%%%

%%%%%%%%%%%%%%%%%%%%%%%%%%%%%%%%%%%%%%%%%%%%%%%%%%%%%%%%%%%%%%%%%%%%%%%%
Input Parameters: NGF/Dextran + Mouse Dual
Conduit %%%%%%%%%%
% conc_reservoir = 25;          %mg/ml
% %time of tests in days
% time_i = 0;
% time_f = 30;
% time_i_hr = time_i*24;
% time_f_hr = time_f*24;
% %number of iterations: over 200 iterations should be accurate to
within .1%
% %cumulative diffusion
% iterations = (time_f_hr-time_i_hr)*2;
% collections = [time_i 1 2 4 7 14 21 28 time_f]; %in days
% no_collect = 0;
% D_coeff_ngf = 1.26e-6;        %cm^2/sec
%
% %hole parameters
% hole_diam = 130;          %um
% hole_count = 1;
%
% %Mouse Dual Conduit size
% %length of reservoir: dual conduit
% res_length = 2;          %mm
% % prompt1 = 'Length of Drug Reservoir (mm)?\n';
% % res_length = input(prompt1);
% %reservoir outer diameter: determined by outer conduit ID
% res_OD = 2.01;          %mm

```

```

% length_IC = 13;          %mm
% receiver_volume = 3;    %ml
% %Stump not used in receiver chamber tests; make dummy variable
% stump_length = 0;      %mm
% %reservoir inner diameter: determined by inner conduit OD
% res_ID = 1.25;         %mm
% %reservoir volume
% reservoir_volume = res_length*pi*((res_OD/2)^2-(res_ID/2)^2); %ul
% fprintf('Reservoir Volume: %.1f ul \n\n', reservoir_volume)
% reservoir_volume = reservoir_volume*.001; %ul
to ml
% %conduit inner diameter: matches 19G needle OD
% conduit_ID = 1.067;    %mm
% thickness_IC = (res_ID-conduit_ID)/2; %mm
%%%%%%%%%%%%%%%%%%%%%%%%%%%%%%%%%%%%%%%%%%%%%%%%%%%%%%%%%%%%%%%%%%%%%%%%

%%% Target Parameters %%%
%target range for accurate Dextran reading: 1000-50000 ng/ml, most
%accurate between 1000-12,500 ng/ml

%target range for accurate NGF reading: .5-20 ng/ml, most
%accurate between 2-10 ng/ml
%%%%%%%%%%%%%%%%%%%%%%%%%%%%%%%%%%%%%%%%%%%%%%%%%%%%%%%%%%%%%%%%%%%%%%%%

%use receiver chamber model of Fick's Diffusion
receiver_model = 0;
[conc_Receiver_all, conc_Receiver_collections, conc_cumulative,
collect_time] = Ficks_Diffusion(receiver_model,...
    D_coeff_ngf, conc_reservoir, thickness_IC, length_IC, time_i_hr,
time_f_hr, iterations, ...
    collections, reservoir_volume, hole_diam, hole_count, conduit_ID,
receiver_volume, stump_length);

%convert NGF/Dextran concentrations to ng/ml from mg/ml
conc_Receiver_all = conc_Receiver_all.*1e6;
conc_Receiver_collections = conc_Receiver_collections.*1e6;
conc_cumulative = conc_cumulative.*1e6;

%array of time values used in model
time = linspace(time_i_hr, time_f_hr, iterations);
collect_time_hr = collect_time/60/60;
time_day = time/24;
collect_time_day = collect_time_hr/24;

%concentration plot
figure(1)
main = plot(time_day, conc_Receiver_all, 'r-');
hold on
plot(collect_time_day, conc_Receiver_collections, 'k*')
cumulative = plot(time_day, conc_cumulative, 'b-');
title('Diffusion Model Release through Guidance Conduit', 'fontweight',
'bold')
xlabel('Time [Days]')
ylabel('Concentration [ng/mL]')

```

```

legend([main cumulative], 'Sample Collections', 'Cumulative Release',
'Location', 'NorthWest');
hold off

%compute percent release
reservoir_mass = reservoir_volume*conc_reservoir*1e6; %ng
receiver_mass = conc_Receiver_all.*receiver_volume; %ng
collection_mass = conc_Receiver_collections.*receiver_volume; %ng
cumulative_mass = conc_cumulative.*receiver_volume; %ng

data_percent = receiver_mass./reservoir_mass*100;
collection_percent = collection_mass./reservoir_mass*100;
cumulative_percent = cumulative_mass./reservoir_mass*100;

%Percent release plots
figure(2)
main = plot(time_day, data_percent, 'r-');
hold on
ylim([0 100])
plot(collect_time_day, collection_percent, 'k*')
cumulative = plot(time_day, cumulative_percent, 'b-');
title('Diffusion Model Percent Release through Guidance Conduit',
'fontweight', 'bold'); %, 'fontsize', 12)
xlabel('Time [Days]')
ylabel('Percent Release [%]')
legend([main cumulative], 'Sample Collections', 'Cumulative Release',
'Location', 'NorthWest');
hold off

%Print collection concentrations
collection_array = [collections; conc_Receiver_collections];
fprintf('Collections for %.fx-%.fum hole(s):\n(For NGF: must remain
between 1000-65000 ng/ml for accurate readings):\n', hole_count,
hole_diam)
fprintf('Day %.f: %.1f ng/ml\n', collection_array);
fprintf('\n')

%%%%%%%%%%%%%%%%%%%%%%%%%%%%%%%%%%%%%%%%%%%%%%%%%%%%%%%%%%%%%%%%%%%%%%%%%% Testing for varying iteration counts %%%%%%%%%%%
% iterations2 = 3;
% [ngf_NoCollect_all2, ngf_Receiver_collections2, collect_time2] =
Ficks_Diffusion(receiver_model,...
% D_coeff_ngf, conc_reservoir, thickness_IC, length_IC, time_i_hr,
time_f_hr, iterations2, ...
% no_collect, reservoir_volume, hole_diam, hole_count, conduit_ID,
receiver_volume, stump_length);
% ngf_NoCollect_all2 = ngf_NoCollect_all2.*1e6;
% time2 = linspace(time_i_hr, time_f_hr, iterations2);
% time_day2 = time2/24;
%
% iterations3 = 10;
% [ngf_NoCollect_all3] = Ficks_Diffusion(receiver_model,...
% D_coeff_ngf, conc_reservoir, thickness_IC, length_IC, time_i_hr,
time_f_hr, iterations3, ...
% no_collect, reservoir_volume, hole_diam, hole_count, conduit_ID,
receiver_volume, stump_length);
% ngf_NoCollect_all3 = ngf_NoCollect_all3.*1e6;
% figure(1)

```

```

% time3 = linspace(time_i_hr, time_f_hr, iterations3);
% time_day3 = time3/24;
%
% iterations4 = 100;
% [ngf_NoCollect_all4] = Ficks_Diffusion(receiver_model,...
%     D_coeff_ngf, conc_reservoir, thickness_IC, length_IC, time_i_hr,
time_f_hr, iterations4, ...
%     no_collect, reservoir_volume, hole_diam, hole_count, conduit_ID,
receiver_volume, stump_length);
% ngf_NoCollect_all4 = ngf_NoCollect_all4.*1e6;
% time4 = linspace(time_i_hr, time_f_hr, iterations4);
% time_day4 = time4/24;
%
% figure(1)
% hold on
% data2 = plot(time_day2, ngf_NoCollect_all2, 'm-');
% data3 = plot(time_day3, ngf_NoCollect_all3, 'c-');
% data4 = plot(time_day4, ngf_NoCollect_all4, 'g-');
% legend([main noreset data2 data3 data4], 'Collections: 0, 1, 3, 7,
14, 21, 28',...
%     'Iterate every minute (43,000)', '3 iterations', '10
iterations',...
%     '100 iterations', 'Location', 'NorthWest')
% hold off
%%%%%%%%%%%%%%%%%%%%%%%%%%%%%%%%%%%%%%%%%%%%%%%%%%%%%%%%%%%%%%%%%%%%%%%%

```

In vivo Release Parameters

The following code is the script that takes input parameters for the nerve conduit, runs the diffusion model, and outputs collection concentrations and plots over time for *in vivo* modelling.

```

%
% Diffusion_NGF_invivo.m
%
% Scott Ho
% Created: 5/8/14
%
% Diffusion Modelling: Model used to determine proper hole sizes and
% expected diffusion rate for in-vivo diffusion. Plotted concentration
is
% the concentration exhibited at the exit of the diffusion hole.
%
%% NGF/Dextran Parameters

% NGF/Dextran: molecule size chosen by matching diffusion coefficient
with NGF
% coefficient.

%%%%%%%%%% Input Parameters: NGF/Dextran + Rat Single
Conduit %%%%%%%%%%

```

```

conc_reservoir = .0001;           %mg/ml
%time of tests in days
time_i = 0;
time_f = 30;
time_i_hr = time_i*24;
time_f_hr = time_f*24;
%number of iterations: over 200 iterations should be accurate to
within .1%
%cumulative diffusion; for under 1% collection error, use 400+
%iterations
iterations = (time_f_hr-time_i_hr)*2;
collections = linspace(0,60,16);   %in days
no_collect = 0;
D_coeff_ngf = 1.26e-6;   %cm^2/sec

%hole parameters
hole_diam = 130;           %um
hole_count = 1;

%Rat Single Conduit size
%length of reservoir: dual conduit
res_length = 7;           %mm
% prompt1 = 'Length of Drug Reservoir (mm)?\n';
% res_length = input(prompt1);
%reservoir outer diameter: determined by outer conduit ID
res_OD = 3.0;             %mm
length_IC = 13/2;        %mm
receiver_volume = 3;      %ml
%Stump not used in receiver chamber tests; make dummy variable
stump_length = 0;        %mm
%reservoir inner diameter: determined by inner conduit OD
res_ID = 2.3;             %mm
%reservoir volume
reservoir_volume = res_length*pi*((res_OD/2)^2-(res_ID/2)^2);   %ul
fprintf('Reservoir Volume: %.1f ul \n\n', reservoir_volume)
reservoir_volume = reservoir_volume/1000;   %ul to ml
%conduit inner diameter: matches 14G needle OD
conduit_ID = 2.01;        %mm
thickness_IC = (res_ID-conduit_ID)/2;      %mm

%calculate diffusion resistances
%R1 = hole resistance
R1 = thickness_IC/(pi*(hole_diam/1000/2)^2*hole_count);
%R2 = inner conduit length to end from diffusion hole(s)
R2 = length_IC/(pi*(conduit_ID/2)^2);
%%%%%%%%%%%%%%%%%%%%%%%%%%%%%%%%%%%%%%%%%%%%%%%%%%%%%%%%%%%%%%%%%%%%%%%%%%%%%%
%%

%%%%%%%%%%%%%%%%%%%%%%%%%%%%%%%%%%%%%%%%%%%%%%%%%%%%%%%%%%%%%%%%%%%%%%%%%%%%%%
Input Parameters: NGF/Dextran + Mouse Dual
Conduit %%%%%%%%%%%
% conc_reservoir = .0001;           %mg/ml
% %time of tests in days
% time_i = 0;
% time_f = 30;
% time_i_hr = time_i*24;
% time_f_hr = time_f*24;

```

```

% %number of iterations: over 200 iterations should be accurate to
within .1%
% %cumulative diffusion
% iterations = (time_f_hr-time_i_hr)*2;
% collections = [time_i .0833 .2917 .75 2 4.9167 11.9167 20 27
time_f];      %in days
% no_collect = 0;
% D_coeff_ngf = 1.26e-6;      %cm^2/sec
%
% %hole parameters
% hole_diam = 32;      %um
% hole_count = 1;
%
% %Mouse Dual Conduit size
% %length of reservoir: dual conduit
% res_length = 2;      %mm
% % prompt1 = 'Length of Drug Reservoir (mm)?\n';
% % res_length = input(prompt1);
% %reservoir outer diameter: determined by outer conduit ID
% res_OD = 2.01;      %mm
% length_IC = 13;      %mm
% receiver_volume = 3; %ml
% %Stump not used in receiver chamber tests; make dummy variable
% stump_length = 0;      %mm
% %reservoir inner diameter: determined by inner conduit OD
% res_ID = 1.25;      %mm
% %reservoir volume
% reservoir_volume = res_length*pi*((res_OD/2)^2-(res_ID/2)^2); %ul
% fprintf('Reservoir Volume: %.1f ul \n\n', reservoir_volume)
% reservoir_volume = reservoir_volume*.001; %ul
to ml
% %conduit inner diameter: matches 19G needle OD
% conduit_ID = 1.067;      %mm
% thickness_IC = (res_ID-conduit_ID)/2; %mm
%
% %calculate diffusion resistances
% %R1 = hole resistance
% R1 = thickness_IC/(pi*(hole_diam/1000/2)^2);
% %R2 = inner conduit length to end from diffusion hole(s)
% R2 = length_IC/(pi*(conduit_ID/2)^2);
%%%%%%%%%%%%%%%%%%%%%%%%%%%%%%%%%%%%%%%%%%%%%%%%%%%%%%%%%%%%%%%%%%%%%%%%
%

%use receiver chamber model of Fick's Diffusion
invivo_model = 1;
[conc_out_all, conc_Receiver_collections, conc_cumulative,
collect_time, conc_conduit,...
    ngf_conduit, ngf_out_all] = Ficks_Diffusion(invivo_model,
D_coeff_ngf,...
    conc_reservoir, thickness_IC, length_IC, time_i_hr, time_f_hr,
iterations,...
    collections, reservoir_volume, hole_diam, hole_count, conduit_ID,
receiver_volume, stump_length);

```

```

%convert NGF/Dextran concentrations to ng/ml from mg/ml
conc_out_all = conc_out_all.*1e6;
conc_Receiver_collections = conc_Receiver_collections.*1e6;
conc_conduit = conc_conduit*1e6;

%array of time values used in model
time = linspace(time_i_hr, time_f_hr, iterations);
collect_time_hr = collect_time/60/60;
time_day = time/24;
collect_time_day = collect_time_hr/24;

%Plot conduit concentration at the diffusion hole exit
figure(1)
main = plot(time_day, conc_conduit, 'r-');
hold on
title('Drug Concentration Within Guidance Conduit', 'fontweight',
'bold')
xlabel('Time [Days]')
ylabel('Concentration [ng/mL]')
% legend([main noreset], 'Sample Collections', 'Cumulative Release',
'Location', 'NorthWest');
hold off

%compute percent release
reservoir_mass = conc_reservoir*reservoir_volume*1e6;    %ng
mass_out =
ngf_out_all*1e6;                                         %ng
%ng

mass_percent = mass_out./reservoir_mass*100;

%Cumulative Percent release plot
figure(2)
percent = plot(time_day, mass_percent, 'r-');
hold on
ylim([0 100])
title('Drug Percent Release from Guidance Conduit', 'fontweight',
'bold'); %, 'fontsize', 12)
xlabel('Time [Days]')
ylabel('Cumulative Release [%]')
legend('Percent Release', 'Location', 'NorthWest');
hold off

%Cumulative Mass release per day
figure(3)
mass_day = plot(time_day, mass_out./time_day, 'r-');
hold on
set(gca, 'YTickLabel', num2str(get(gca, 'YTick'))))
title('Drug Mass Release from Guidance Conduit', 'fontweight',
'bold'); %, 'fontsize', 12)
xlabel('Time [Days]')
ylabel('Cumulative Release [ng/day]')
legend('Mass Release per Day', 'Location', 'NorthEast');
hold off

%Cumulative Percent release per day
figure(4)

```

```

percent_day = plot(time_day, mass_percent./time_day, 'r-');
hold on
title('Drug Percent Release from Guidance Conduit', 'fontweight',
'bold'); %, 'fontsize', 12)
xlabel('Time [Days]')
ylabel('Cumulative Release [%/day]')
legend('Percent Release per Day', 'Location', 'NorthEast');
hold off

%Print collection concentrations
collection_array = [collections; conc_Receiver_collections];
fprintf('Collections for %.fx-%.fum hole(s):\n(For NGF: must remain
between 1000-65000 ng/ml for accurate readings):\r', hole_count,
hole_diam)
fprintf('Day %.f: %.1f ng/ml\r', collection_array);
fprintf('\n')

```


REFERENCES

- [1] M. G. Burnett and E. L. Zager, "Pathophysiology of Peripheral Nerve Injury: A Brief Review," *Neurosurgical Focus*, vol. 16, no. 5, 2004.
- [2] J. G. Boyd and T. Gordon, "Neurotrophic Factors and Their Receptors in Axonal Regeneration and Functional Recovery After Peripheral Nerve Injury," *Molecular Neurobiology*, vol. 27, no. 3, pp. 277-324, 2003.
- [3] E. G. Fine, I. Decosterd, M. Papaloizos, A. D. Zurn and P. Aebischer, "GDNF and NGF Released by Synthetic Guidance Channels Support Sciatic Nerve Regeneration Across a Long Gap," *European Journal of Neuroscience*, vol. 15, pp. 589-601, 2002.
- [4] A. C. Lee, V. M. Yu, J. B. Lowe III, M. J. Brenner, D. A. Hunter, S. E. Mackinnon and S. E. Sakiyama-Elbert, "Controlled Release of Nerve Growth Factor Enhances Sciatic Nerve Regeneration," *Experimental Neurology*, vol. 184, pp. 295-303, 2003.
- [5] S. Madduri, M. Papaloizos and B. Gander, "Synergistic Effect of GDNF and NGF on Axonal Branching and Elongation In Vitro," *Neuroscience Research*, vol. 65, no. 1, pp. 88-97, 2009.
- [6] X. Navarro, E. Udina, D. Ceballos and B. G. Gold, "Effects of FK506 on Nerve Regeneration and Reinnervation After Graft or Tube Repair of Long Nerve Gaps," *Muscle and Nerve*, vol. 24, no. 7, pp. 905-915, 2001.
- [7] F. J. Rodriguez, E. Verdu, D. Ceballos and X. Navarro, "Nerve Guides Seeded with Autologous Schwann Cells Improve Nerve Regeneration," *Experimental Neurology*, vol. 161, no. 2, pp. 571-584, 2000.
- [8] J. Terzis, D. Sun and P. Thanos, "Historical and Basic Science Review: Past, Present, and Future of Nerve Repair," *Reconstructive Microsurgery*, vol. 13, pp. 215-225, 1997.
- [9] J. Hu, Q.-T. Zhu, X.-L. Liu and J.-K. Zhu, "Repair of Extended Peripheral Nerve Lesions in Rhesus Monkeys Using Acellular Allogenic Nerve Grafts Implanted with Autologous Mesenchymal Stem Cells," *Experimental Neurology*, vol. 204, pp. 658-666, 2007.

- [10] G. Lundborg, R. H. Gelberman, F. M. Longo, H. C. Powell and S. Varon, "In Vivo Regeneration of Cut Nerves Encased in Silicone Tubes: Growth Across a Six-millimeter Gap," *Journal of Neuropathology and Experimental Neurology*, vol. 41, no. 4, pp. 412-422, 1982.
- [11] J. Stammen, S. Williams, D. Ku and R. Guldberg, "Mechanical Properties of a Novel PVA Hydrogel in Shear and Unconfined Compression.," *Biomaterials*, vol. 22, no. 8, pp. 799-806, 2001.
- [12] S. Kehoe, X. Zhang and D. Boyd, "FDA Approved Guidance Conduits and Wraps for Peripheral Nerve Injury.," *Injury*, vol. 43, no. 5, pp. 553-572, 2012.
- [13] H. K. Makadia and S. J. Siegel, "Poly Lactic-co-Glycolic Acid (PLGA) as Biodegradable Controlled Drug Delivery Carrier," *Polymers (Basel)*, vol. 3, no. 3, pp. 1377-1397, 2012.
- [14] A. R. Nectow, K. G. Marra and D. L. Kaplan, "Biomaterials for the Development of Peripheral Nerve," *Tissue Engineering*, vol. 18, no. 1, pp. 40-50, 2012.
- [15] P. Gentile, V. Chiono, I. Carmagnola and P. V. Hatton, "Review of Poly(lactic-co-glycolic) Acid (PLGA)-based Materials for Bone Tissue Engineering," *Int. J. Mol. Sci.*, vol. 15, no. 3, pp. 3640-3659, 2014.
- [16] R. A. Miller, J. M. Brady and D. E. Cutright, "Degradation Rates of Oral Resorbable Implants (Polylactates and Polyglycolates): Rate Modification with Changes in PLA/PGA Copolymer Ratios," *Journal of Biomedical Materials Research*, vol. 11, no. 5, pp. 711-719, 1977.
- [17] K.-M. Lin, "Implantable Devices for Sensing and Drug Delivery in Ophthalmology and Reconstructive Surgery," *PhD Dissertation, Dept. Mech. Eng., Univ. of Utah, Salt Lake City, UT*, 2014.
- [18] M. Stroh, W. R. Zipfel, R. M. Williams, W. W. Webb and W. M. Saltzmann, "Diffusion of Nerve Growth Factor in Rat Striatum as Determined by Multiphoton Microscopy," *Biophysical Journal*, vol. 85, no. 1, pp. 581-588, 2003.
- [19] C. E. Holy, C. Cheng, J. E. Davies and M. S. Shoichet, "Optimizing the Sterilization of PLGA Scaffold for Use in Tissue Engineering," *Biomaterials*, vol. 22, no. 1, pp. 25-31, 2001.
- [20] M. Eng, V. Ling, J. A. Briggs, K. Sousa, E. Canova-Davis, M. F. Powell and L. R. De Young, "Formulation Development and Primary Degradation Pathways for Recombinant Human Nerve Growth Factor.," *Analytical Chemistry*, vol. 69, no. 20, pp. 4184-4190, 1997.

- [21] H. K. Makadia and S. J. Siegel, "Poly Lactic-co-Glycolic Acid (PLGA) as Biodegradable Controlled Drug Delivery Carrier," *Polymers*, vol. 3, pp. 1377-1397, 2011.
- [22] G. Evans, K. Brandt, M. Widmer, L. Lu, R. Meszlenyi, P. Gupta, A. Mikos, J. Hodges, J. Williams, A. Gurlek, A. Nabawi, R. Lohman and C. Patrick Jr., "In Vivo Evaluation of Poly(L-Lactic Acid) Porous Conduits for Peripheral Nerve Regeneration," *Biomaterials*, vol. 20, no. 12, pp. 1109-1115, 1999.